Aus der Abteilung für experimentelle Neurologie

der Medizinischen Fakultät Charité – Universitätsmedizin Berlin

DISSERTATION

Generation of Monoclonal Antibodies against the Metabotropic Glutamate Receptor 5 and Progranulin in Autoimmune Encephalitis and a Potential Approach to Remedy Antibody Effects

zur Erlangung des akademischen Grades Doctor medicinae (Dr. med.)
vorgelegt der Medizinischen Fakultät

Charité – Universitätsmedizin Berlin

von Sarah Lina Kurpjuweit

aus Herbolzheim

Datum der Promotion: 17.September 2021

Table of Contents

Abbreviations

AMPAR *α-amino-3-hydroxy-5-methyl-4-isoxazolepropionic acid receptor*

ASC *Antibody-secreting cell*

BSA *Bovine serum albumin*

CASPR2 *Contactin-associated protein-like 2*

CDR3l *CDR3 length*

CNS *Central nervous system*

CSF *Cerebrospinal fluid*

DMEM *Dulbecco's Modified Eagle Medium*

DMSO *Dimethylsulfoxid*

dNTP *deoxyribonucleotide triphosphate*

DPPX *dipeptidyl-peptidase-like protein-6*

DTT *Dithiothreitol*

ELISA *Enzyme-linked Immunosorbent Assay*

F *Function*

FACS *Fluorescence-activated cell sorting*

FCS *Fetal calf serum*

GABAR *gamma-aminobutyric acid receptors*

GAD *glutamic acid decarboxylase*

H *Heavy*

HEK cells *Human embryonic kidney cells*

Ig *Immunoglobulin*

K *Kappa*

L *Lambda*

LGI1 *Leucine Rich Glioma Inactivated 1*

MBC *Memory b cell*

mGluR1 *metabotropic glutamate receptor 1*

mGluR5 *Metabotropic glutamate receptor 5*

NGS *Normal goat serum*

nMBC *Non-memory b cell*

NMDAR N-methyl-D-aspartate receptor

PCR *Polymerase chain reaction*

RHP *Random hexamer primers*

Register of Figures

Register of Tables

Abstract

Within the last years, autoimmune encephalitis has become a novel disease group in neurology. The rapidly growing number of newly identified autoantibodies reactive to the central nervous system (CNS) in patients with well-defined clinical syndromes indicate a likelihood of yet broad underestimation of autoimmune pathomechanisms in clinical routines. Diagnostics are still based on testing patient serum or cerebrospinal fluid (CSF) as a whole and the contribution of individual immune cells or antibodies remain unknown although a deeper understanding of underlying cellular and molecular disease mechanisms is indispensable to further develop diagnostic and therapeutic strategies.

We therefore strived to isolate single memory B cells (MBCs), non-memory B cells (nMBCs) and antibody-secreting cells (ASCs) out of CSF samples from patients with proven autoreactivity against metabotropic glutamate receptor 5 (mGluR5) or Progranulin with fluorescence-activated single cell sorting. We proposed generating recombinant monoclonal antibodies based on these cells, carrying out a multi-step protocol including polymerase chain reactions (PCRs), sequence analysis, cloning and expression of antibodies in human embryonic kidney cells (HEK cells). To identify clones binding to mGluR5 and Progranulin, respectively, generated antibodies were tested on murine brain slices and in cell-based assays. Furthermore, Fab antibody fragments were created and tested for their ability to displace harmful full antibodies on murine brain sections.

We succeeded in cloning cells from CSF samples and proved reactivity against mGluR5 for five recombinant monoclonal antibodies, albeit for none against Progranulin. We provide a characterization of this polyclonal immune response against mGluR5 including genetic information about the reactive clones. Moreover, we describe various other reactivities identified among the monoclonal antibodies. We demonstrate that Fab fragments can displace full IgG antibodies with identical antigen-binding sites and are therefore a useful scientific tool for investigation of antibody effects and may even have some potential to remedy noxious antibody effects.

Overall we provide a deeper understanding of the immune response in the context of autoimmune encephalitis with reactivity against mGluR5 and Progranulin, respectively. We not only provide theoretical information but also enable thorough investigation of disease mechanisms by supplying monoclonal antibodies for in-depth testing. We furthermore pave the way for investigating Fab fragments for a possible therapeutic potential in autoimmune encephalitis.

Zusammenfassung

In den letzten Jahren hat sich das Spektrum der autoimmunen Enzephalitiden als eine neue Erkrankungsgruppe in der Neurologie etabliert. Die schnell wachsende Anzahl an neu identifizierten ZNS-reaktiven Autoantikörpern bei Patienten mit gut umschriebenen klinischen Syndromen legt nahe, dass die Rolle autoimmuner Pathomechanismen im klinischen Alltag noch immer deutlich unterschätzt wird. Diagnostische Verfahren stützen sich noch immer auf die Untersuchung von Serum oder Liquor als Gesamtprobe und die Rolle einzelner zellulärer Komponenten und Antikörper bleibt unklar, obwohl ein tiefgreifenderes Verständnis für zugrundeliegende zelluläre und molekulare Mechanismen notwendig ist um Strategien für Diagnostik und Therapie weiterzuentwickeln.

Unser Ziel war es daher, mittels Fluoreszenz-aktivierter Einzelzellsortierung CD27-positive und CD27-negative B-Zellen, sowie Antikörper-sezernierende Zellen aus Liquorproben von Patienten mit nachgewiesener Auto-Reaktivität gegen mGluR5 oder Progranulin zu isolieren. Wir führten ein mehrschrittiges Protokoll durch, welches Polymerase-Kettenreaktionen, Sequenzanalysen, Klonierung und die Expression von rekombinanten monoklonalen Antikörpern in HEK-Zellen umfasst. Um jene Klone zu identifizieren, die die gesuchte Reaktivität gegen mGluR5 beziehungsweise Progranulin aufweisen, testeten wir die generierten Antikörper auf Maushirnschnitten und transfizierten HEK-Zellen. Darüber hinaus untersuchten wir, ob Fab-Antikörperfragmente schädliche Antikörper im Rahmen einer autoimmunen Enzephalitis verdrängen können.

Wir isolierten erfolgreich Zellen aus den Liquorproben der Patienten und bewiesen für fünf derer rekombinanten monoklonalen Antikörper eine Reaktivität gegen mGluR5, konnten jedoch keine Progranulin-reaktiven Antikörper generieren. Wir charakterisieren hier diese polyklonale Immunantwort gegen mGluR5 unter Analyse der genetischen Informationen der reaktiven Klone. Auch konnten wir andere Reaktivitäten der isolierten Zellen rekonstruieren und stellen diese dar. Des Weiteren zeigen wir, dass Fab-Antikörperfragmente ein nützliches Tool zur Untersuchung von Antikörpereffekten sind und mit ganzen Antikörpern um Bindungsstellen konkurrieren, wodurch sie möglicherweise auch ein gewisses Potential aufweisen, Effekte schädlicher Antikörper abzuwenden.

Zusammenfassend ermöglichen wir mit dieser Arbeit ein tiefgreifenderes Verständnis für die Immunreaktion im Rahmen einer autoimmunen Enzephalitis gegen mGluR5 beziehungsweise Progranulin. Wir stellen hierbei nicht nur theoretische Informationen zur Verfügung, sondern ermöglichen mit unseren monoklonalen Antikörpern weiterführende Experimente um Pathomechanismen zu untersuchen. Wir ebnen außerdem den Weg um ein mögliches therapeutisches Potential von Fab-Antikörperfragmenten für autoimmune Enzephalitiden zu untersuchen.

1 Introduction

1.1 The Spectrum of Autoimmune Encephalitis

Within the last years, autoimmune encephalitis has become a novel disease group in neurology. The rapidly growing number of newly identified autoantibodies in patients with well-defined clinical syndromes targeting a variety of central nervous system (CNS) cell surface antigens indicate that a considerable underestimation in clinical routines is still likely. (Esposito et al., 2019; Guan et al., 2016). Even though detection rates have multiplied within the last two decades, identifying patients with autoimmune encephalitis remains a challenge due to heterogeneity in clinical presentation (Dubey et al., 2018). Furthermore, existing diagnostic criteria for encephalitis are often based on characteristics of infectious encephalitis and therefore prone to miss cases with non-infectious pathogeneses as they can lack fever or elevated cell counts in the cerebrospinal fluid (CSF) (Leypoldt et al., 2015). As one of the most rapidly changing areas in neurology, the spectrum of autoimmune encephalitis has broadened from the archetypal anti-NMDAR encephalitis to forms with antibodies against numerous other epitopes. Most commonly, autoantibodies in autoimmune encephalitis are directed against N-methyl-D-aspartate receptor (NMDAR), α-amino-3-hydroxy-5-methyl-4-isoxazolepropionic acid receptor (AMPAR), both type A and B of gamma-aminobutyric acid receptors (GABAR), Leucine Rich Glioma Inactivated 1 (LGI1), Contactin-associated protein-like 2 (CASPR2), dipeptidyl-peptidase-like protein-6 (DPPX), Glycine receptor, metabotropic glutamate receptor 1 (mGluR1) and metabotropic glutamate receptor 5 (mGluR5), Dopamine-2-receptor, Amphiphysin and glutamic acid decarboxylase (GAD) (Dalmau & Rosenfeld, 2014).

Dalmau and Rosenfeld (2014) suggest a system to integrate this new category of autoantigens into the large group of autoimmune encephalitis: in contrast to the classical paraneoplastic antibodies that have been described, such as anti-Hu, anti-Yo, anti-Ri, anti-Cv2/CRMP5, anti-Ma, anti-recoverin or anti-Tr antibodies which commonly target intracellular epitopes within the CNS, the novel encephalitis autoantibodies bind to surface antigens or synaptic proteins, which means that they can target their epitope directly. Due to this binding to direct effectors such as receptors and synaptic proteins, these antibodies can initiate pathological mechanisms immediately (Dalmau & Rosenfeld, 2014). But this new type of autoimmune encephalitis and classic paraneoplastic encephalitis diverge not only concerning the type of antigens they target; epidemiological data reveals patients with autoimmune encephalitis to be younger and their

occurrence in conjunction with a malignant comorbidity is less common (Darnell & Posner, 2011 and Eric Lancaster et al., 2011 as cited in Dalmau & Rosenfeld, 2014).

There is heterogeneous literature suggesting altered classifications for different types of autoimmune encephalitis. With ongoing research and extension of this spectrum of disease, new epitopes will be characterized. The dissertation focuses on two antigens associated with autoimmune encephalitis; one of them, mGluR5, can be classified within the group of surface receptors. The second antigen of interest, progranulin, is far less common in the context of autoimmune encephalitis. Anti-Progranulin encephalitis has not yet been described as an entity itself, but the function of Progranulin is being investigated in connection with various neurological disorders, which begs the question of its role in autoimmune encephalitis.

1.2 mGLuR5 and Encephalitis

Besides the ionotropic glutamate receptors such as the NMDAR as the archetypical antigen in autoimmune encephalitis, there is a group of metabotropic glutamate receptors which on activation do not lead to electrical changes through immediate ion flow, but initiate intracellular pathways (Gregory et al., 2013; Zhou & Danbolt, 2014). Among this group, mGluR5 has been described as a target in autoimmune encephalitis (Spatola et al., 2018). This receptor converts signals from the extracellular space into intracellular signaling, which results in Ca^{2+} changes as are characteristic for G-protein-coupled receptors (Sergin et al. 2017). Within the cells, its translocation to the inner nuclear membrane has been demonstrated (Sergin et al., 2017). The major pathway leads through $G\alpha_{q/11}$ proteins, phospholipase Cβ1, diacylglycerol and inositol-1,4,5-triphosphate to activation of protein kinase C and finally to Ca^{2+} shifts, but more complex pathways upon activation of mGluR5, for instance, involve Homer1b/c (Mao et al., 2005). Expression of mGluR5 is highest in the hippocampus, dorsal striatum, cerebral cortex and thalamus (Cai et al., 2019; Romano et al., 1995).

mGluR5 has been discussed in the context of a variety of neurological and psychiatric disorders. Among others, there is evidence for its role in Alzheimer's disease, Parkinson's disease, Huntington's disease, schizophrenia and stress disorders (Esterlis et al., 2018; Kumar et al., 2015; Oertel & Schulz, 2016; H.-Y. Wang et al., 2018; Ribeiro et al., 2010).

Spatola et al. (2018) have characterized cases of anti-mGluR5 encephalitis including both children and adults: out of the 11 patients they depict, ten showed altered personality or behavior which in some cases manifested itself as hallucinations or psychosis. Impaired cognition was identified as another common symptom. Seizures, motor deficit and affected consciousness were reported in this study, but they were less common. Furthermore, the medical history of some of these patients revealed prodromes such as headache and nausea. Several of the patients included reported weight loss, although demarcation from symptoms of coexisting malignant disease is difficult. (Spatola et al., 2018)

When intertwined with Hodgkin lymphoma, presence of effective antibodies against mGluR5 with corresponding clinical features is referred to as "Ophelia syndrome" (Carr, 1982; Mat et al., 2013). Due to the limited number of cases identified, there is not yet an established therapy regime specific to anti-mGluR5 encephalitis. However, treatment approaches have been similar to those for related disorders such as anti-NMDAR encephalitis and have included corticosteroids, plasma exchange and application of intravenous immunoglobulin (Ig) (Dalmau & Rosenfeld, 2014).

1.3 Progranulin and Encephalitis

Progranulin is a secreted glycoprotein that has effects on inflammatory processes both as a whole and fragmented into particles called granulins (Kao et al., 2017). Formerly known as proepithelin, acrogranin or prostate cancer cell derived growth factor, it also plays a major role in tissue repair and tumorigenesis (He & Bateman, 2003). Encoded by a gene called GRN, it is expressed in numerous types of tissue and can be found in various organs, bone marrow, cells of the immune system and epithelia (Daniel et al., 2000; Bhandari et al., 1992). Progranulin has anti-inflammatory effects and is furthermore known to play a role in carcinogenesis (Cenik et al., 2012). Recently it has been shown to "promote neuronal cell survival" (Ryan et al., 2009). Presence in both CSF and serum has been proven with Enzyme-linked Immunosorbent Assay (ELISA) (Ghidoni et al., 2008). Within the central nervous system the highest expression can be found in neurons and microglia (Petkau et al., 2010; Ryan et al., 2009).

The role of progranulin in the pathogenesis of various neurological disorders is under investigation. It is commonly known that mutations in GRN can lead to frontotemporal lobar degeneration with TDP-43 inclusions (Benussi et al., 2009). Homozygote mutation patterns are

under discussion as leading to neuronal ceroid lipofuscinosis (Smith et al., 2012). However, less linear effects of progranulin need to be investigated in disorders with affected behavior and cognitive function. An earlier study revealed presence and pro-inflammatory effects of antibodies against progranulin in several autoimmune diseases (Thurner et al., 2013). However, there is a lack of published data on a possible role of progranulin and antibodies against it in autoimmune encephalitis. Due to the anti-inflammatory function of progranulin, a pro-inflammatory impact of antibodies against it or a modulation of immune responses in a deviant manner seems probable. With both its increasing significance for the understanding of various neurological disorders and the revealed presence of antibodies against it in several autoimmune diseases, progranulin qualifies as an interesting candidate for our research on epitopes in autoimmune encephalitis.

1.4 Studying B cells and Antibodies in Autoimmunity

1.4.1 B cell Maturation

Melchers (2015) describes the development of B cells as originating from pluripotent hematopoietic stem cells: precursors of B cells first migrate into the fetal liver, and this is followed by maturation of B cells in bone marrow and secondary lymphoid tissue during the entire life span. In early development, he states, variants for V, D and J segments are assorted and rearranged for each cell to build up the basis for forming B cell receptors. Heavy chains containing V, D and J segments are constituted first, with light chains lacking the D segment being matched with them subsequently (Melchers, 2015). Later on these genes can be further developed by introducing somatic hypermutations, multiplying variability to meet as many antigens as possible (Melchers, 2015).

Mature B cells that express IgM and IgD on their surface and that are capable of antigen recognition can be found in the spleen and lymph nodes or on their way between these locations (Cruse & Lewis, 2004). In this state they can be activated by T cells with appropriate co-stimulation to then further develop in follicles in the secondary lymphoid organs, thereby proliferating and differentiating into cells producing antibodies for immediate antigen interaction and memory B cells (Cruse & Lewis, 2004). Antibody-secreting cells result from antigen stimulation and the immunoglobulins they secrete are designated as antibodies (Cruse & Lewis, 2004). Out of the five classes of immunoglobulins, IgM, IgG and IgA make up the

majority, with IgE and IgD representing a minor share (Cruse & Lewis, 2004). The smallest unit of all is constituted of two identical heavy chains and two identical light chains, even though based on this unit, IgM and IgA are the only classes to build multimeric structures (Cruse & Lewis, 2004). With every class of immunoglobulin featuring unique characteristics, IgM is the first type of immunoglobulin expressed upon antigen stimulation (Cruse & Lewis, 2004). Although in theory all immunoglobulins can occur membrane-bound, all but IgD are commonly found detached from the cells they originated from. (Cruse & Lewis, 2004)

Passing through different stages of maturation, B cells express structures on their surface revealing their level of development. These so-called clusters of differentiation (CD) can be of use not only to identify cells of interest, but also to sort them using flow cytometry. While CD19 is expressed during the entire process, CD20 and CD21 are useful for recognzing mature B cells while CD23 is characteristic for activated B cells (LeBien & Tedder, 2008). The expression of CD27 allows differentiation of CD27 positive memory B cells from CD27 negative non-memory B cells (Torigoe et al., 2017). High expression of CD138, also known as syndecan-1, can be found in antibody-secreting cells (Sanderson et al., 1989).

1.4.2 Polyclonality and Polyspecifity

All B cell receptors expressed by one B cell are identical and analogously every plasma cell produces only one type of immunoglobulin and antibody, respectively (Cruse & Lewis, 2004). Still, immune response and concomitant autoimmunity in vivo are significantly more complex due to polyclonality and polyspecifity. Once an antigen has attracted attention, a polyclonal immune response is initiated, involving and enhancing B cells against various epitopes of the antigen. Furthermore, one cell and its immunoglobulins do not have to be specific to one epitope but may interact with different epitopes and different antigens as antibody-antigen interaction is not an absolute lock-and-key system, but is dependent on protein-protein interaction with varying affinities (Van Regenmortel, 2014). Sheer binding of an antibody, can thus, properly speaking, only be an association and not proof of causality (Van Regenmortel, 2014). Therefore we face several limitations when aiming to model in vivo immune response by generating monoclonal antibodies in vitro. On the one hand we have to regard the background of antibodies present but irrelevant for the cause. On the other hand the antibodies we generate can only represent an excerpt of the immune response taking place in vivo.

1.4.3 B cells in Autoimmune Encephalitis

Melchers (2015) illustrates numerous checkpoints throughout B cell development operating in the bone marrow to eliminate B cells with too low, too high or autoreactive affinities. As avoidance of autoimmunity is one of the major goals, heavy chains are first exposed to autoantigens before being reviewed in combination with their corresponding light chains (Melchers, 2015). During these selection processes the number of cells that are allowed passage out of the bone marrow is diminished to a share of approximately 15% of candidates, whereby cells with low affinity to autoantigens are tolerated (Melchers, 2015). Further down the line when maturing in the spleen, autoreactive B cells can be eliminated as their binding to autoantigens at this stage causes anergy or even apoptosis (Rolink et al., 1998). Moreover, several mechanisms for controlling autoreactive cells in the periphery are in place, for instance "inhibitory molecules, anergy, ignorance, and active suppression" (Theofilopoulos et al., 2017). Elimination of autoreactive agents of the immune system is not absolute and their sheer occurrence is a necessary but not sufficient condition to cause pathological autoimmune responses, with vulnerability being predisposed by many factors such as inflammation, tissue damage, genetic loading and environmental influences (Theofilopoulos et al., 2017). Besides these mechanisms to prevent autoimmunity in general, the CNS, hypothetically, has an even lower probability of being attacked: theoretically, the CNS is isolated against activity of the immune system, but it is widely known that there are conditions altering the stability and reliability of the barriers (Daneman & Prat, 2015; Zlokovic, 2008). With the recent characterizations of lymphatic and glymphatic systems in the brain, traditional concepts of a strict immune privilege have to be abandoned (Jessen et al., 2015; Louveau et al., 2015). Furthermore, antibodies cannot only enter the CNS, but are even secreted intrathecally in autoimmune encephalitis (Blinder & Lewerenz, 2019). Three potential ways to enter the CNS are under discussion with respect to the pathogenesis of autoimmune encephalitis: the blood-brain barrier, the blood-cerebro spinal fluid barrier and the olfactory route (Platt et al., 2017).

1.5 Generating Monoclonal Antibodies in Autoimmune Encephalitis

1.5.1 Generating Full IgG Antibodies

Kreye et al. (2016) have already succeeded in creating monoclonal antibodies against the NMDAR and an adjusted protocol was used to investigate anti-LGI1 encephalitis (Kornau et al., 2020). Using CSF samples of patients with autoimmune encephalitis as a starting point, the strategy is based on a protocol introduced by Tiller et al. (2008): applying the lysate of sorted cells as a template, DNA is amplified and cells are cloned to recreate the antibody repertoire of a patient sample. Overall, this process allows the recombinant generation of larger amounts of immunoglobulins, each batch being identical to one cell retrieved from a CSF sample (Tiller et al., 2008). These monoclonal antibodies can subsequently be used for in-depth testing, for instance in cell-based assays, immunohistochemistry and neuronal cell cultures (Kreye et al., 2016). This approach allows a step beyond testing of a CSF sample's reactivity as a whole: analyzing the role of particular cellular components and immunoglobulins, respectively. Established for NMDAR encephalitis, this method can help our understanding of other types of autoimmune encephalitis as well.

1.5.2 Generating Fab Fragments

Besides generating full immunoglobulins, there are many deviating constructs for antibodies. One of these models is Fab fragments, which consist of one shortened heavy chain lacking the Fc part and one full light chain (Cruse & Lewis, 2004; Figure 1). When such Fab fragments were applied in a model of the archetypical anti-NMDAR encephalitis, they did not cause the same pathological effects as full IgG providing identical antigen-binding sites (Hughes et al., 2010). One detrimental effect happening upon binding of full IgG targeting NMDAR but not when applying corresponding Fab fragments was a decrease in NMDAR receptors on the synaptic surface (Hughes et al., 2010). Necessary for this decrease appears to be crosslinking of receptors which can be implemented either by full IgG or by Fab fragments crosslinked by a secondary antibody but not by Fab fragments alone (Hughes et al., 2010). Fab fragments occupying binding sites for autoantibodies without causing the same harmful effects evokes the question of whether they could displace harmful full IgG and therefore may be of therapeutic use. Furthermore, it has yet to be investigated to what extent these findings can be transferred from the archetypical anti-NMDAR encephalitis to other types of autoimmune encephalitis.

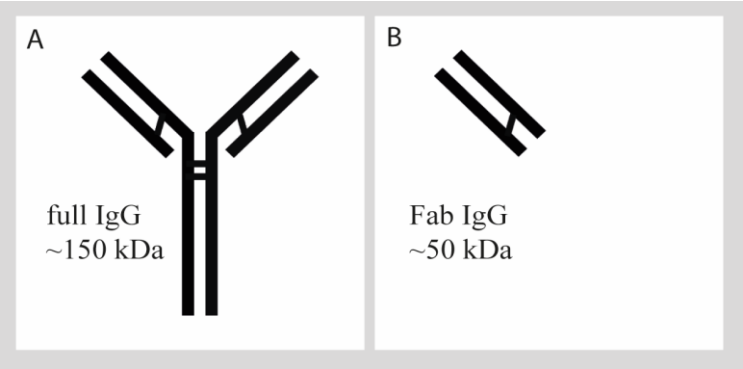

Figure 1: Model of full IgG (A) and Fab fragments (B)

1.6 Goal of this Dissertation

1.6.1 Hypothesis I

Diagnostics for autoimmune encephalitis are commonly based on the reactivity of patient serum or CSF. However, this only allows an observation of the reactivity of the sample as a whole and does not provide any deeper understanding of the contribution of isolated components. We hypothesized that monoclonal antibodies against mGluR5 and Progranulin can be cloned and recombinantly produced from patients with autoreactivity against these two targets. For this purpose, we aimed to isolate single memory B cells (MBCs), non-memory B cells (nMBCs) and antibody-secreting cells (ASCs) binding to mGluR5 from CSF samples with reactivity against mGluR5. Analogously, we aimed to isolate cells binding to Progranulin out of CSF samples with reactivity against Progranulin. We wanted to prove reactivity against mGluR5 and Progranulin, respectively, on a monoclonal level. We proposed creating recombinant monoclonal antibodies against mGluR5 and Progranulin based on these cells, applying a protocol pre-described by Tiller et al. (2008) and making necessary adjustments for our purpose. This process of generating monoclonal antibodies based on sorted single cells also included a step of sequencing the cells' genes encoding for B cell receptors and secreted immunoglobulins, respectively. In doing so, we aimed to analyze the DNA of relevant cells, postulating that effective cells may show certain characteristics regarding immunoglobulin subclass, used V, D and J segments, sequences encoding for the CDR3 region as well as the number and type of somatic hypermutations within the hypervariable regions. Based on this sequencing information, we wanted to identify potential clonal identity and expansion.

1.6.2 Hypothesis II

We hypothesized that we could create Fab fragments featuring antigen-binding sites identical to those contained in the recombinant full IgG antibodies we cloned and that such Fab fragments could displace their corresponding full IgG antibodies. Fab fragments and corresponding full IgG antibodies can be used in experiments enabling further understanding of antibody binding behavior and subsequent disease mechanisms in autoimmune encephalitis. A potential displacement of full IgG antibodies with Fab fragments is of particular interest as Fab fragments have been shown not to cause the same pathological effects as full IgG antibodies in archetypical anti-NMDAR encephalitis (Hughes et al. 2010). Therefore, displacing harmful full IgG with Fab fragments in this case might remedy toxic antibody effects. For other entities of autoimmune encephalitis it is unknown whether pathomechanisms depend on the Fc part contained in full IgG antibodies. The patient-derived Fab fragments we aimed to create could be a scientific tool to reveal which pathomechanisms are Fc-dependent.

2 Methods and Materials

Aiming to analyze the antibody repertoire in the CSF samples available to us, we carried out a protocol that consisted of several steps, leading from CSF samples to monoclonal antibodies, with each batch of monoclonal antibodies representing one cell retrieved from the CSF sample of the patient (Figure 1). The protocol is based on work published by Tiller et al. (2008) and was established in our group by Kreye et al. (2016). This pathway to generating recombinant monoclonal antibodies includes fluorescence-activated cell sorting (FACS) for single cell sorting, a multi-step polymerase chain reaction (PCR) strategy with intermittent sequencing, cloning, transformation into E. coli and transfection of human embryonic kidney cells (HEK cells) in order to finally harvest antibodies from their supernatant (Figure 1). Generating and testing antibodies was performed with Jakob Kreye (DZNE, Charité); he was responsible for the greater part of sample AI-ENC 136, while I was in charge of patient samples AI-ENC 001, AI-ENC 82, AI-ENC 148, AI-ENC 158 and AI-ENC 159.

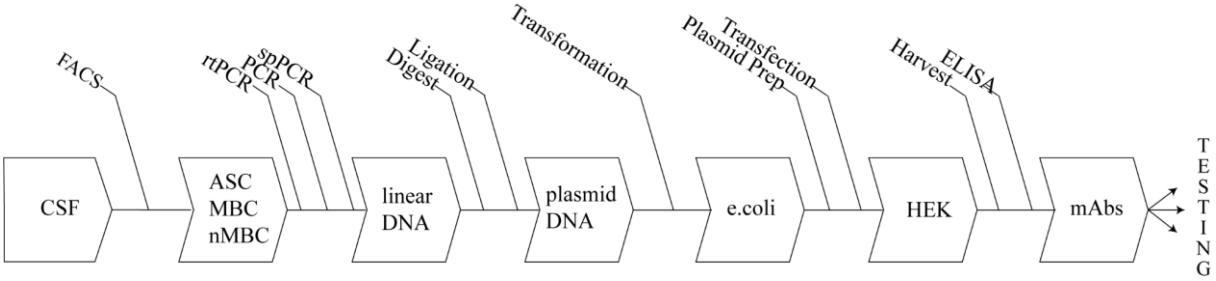

Figure 2: Generating monoclonal antibodies (mAbs)

2.1 Materials

Table 1: Antibodies

Reactivity	Host	Conjugate	Manufacturer	ID
CD3	Mouse	FITC	Miltenyi Biotec	130-098-162
CD14	Mouse	FITC	Miltenyi Biotec	130-098-063
CD16	Mouse	FITC	Miltenyi Biotec	130-098-099
CD20	Mouse	PerCP-Vio700	Miltenyi Biotec	130-100-435
CD27	Mouse	APC-Vio700	Miltenyi Biotec	130-098-605
CD138	Mouse	PE	Miltenyi Biotec	130-098-122
FLAG	Rat	Alexa Fluor 488	Invitrogen	MA1-142-A488
FLAG	Mouse	-	Sigma-Aldrich	F1804
Progranulin	Mouse	-	Adipogen	AG-20A-0052
MAP2	Chicken	-	Invitrogen	PA1-16751
Human IgG	goat	Alexa Fluor 488	Dianova	109-545-003
Mouse IgG	goat	Alexa Fluor 594	Dianova	115-585-003
Chicken IgG	goat	Alexa Fluor 568	Invitrogen	AB_2534098

Table 2: Plasmids

Plasmid	Manufacturer	ID
mGLuR5-FLAG	GenScript	NM_000842
Progranulin-GFP	Sino Biological	HG10826-ACG

Table 3: Kits

Application	Manufacturer	ID
NucleoSpin PCR Clean-Up and Gel Extraction	Macherey-Nagel	740609.50
NucleoSpin PCR Clean-Up 96-well	Macherey-Nagel	740658.4
NucleoSpin Plasmid QuickPure	Macherey-Nagel	740615.50
NucleoSpin Plasmid QuickPure 96-well	Macherey-Nagel	740491.4
NucleoBond® Xtra Maxi Plasmid Purification	Macherey-Nagel	740424.50
Human IgG ELISA	Mabtech	3850-1AD-6

Table 4: Equipment and supplies

Application	Manufacturer	ID
Protein G Sepharose® beads	GE Healthcare	17-0618-01
Chromatography columns	BioRad	732-6008
Amicon Ultra-0.5 Centrifugal Filter Unit (10 kDa)	Millipore	Z677108-96EA
Amicon Ultra-0.5 Centrifugal Filter Unit (100 kDa)	Millipore	UFC510024
Anti-FLAG M2 Magnetic beads	Millipore	M8823

Table 5: Software

Program	Usage
FlowJo	FACS
Microsoft Office	Text and data processing
Adobe Illustrator	Image processing, graphs
Adobe Photoshop	Image processing
Snapp gene	Sequence analysis
Sequence Scanner	Sequence analysis

Table 6: Chemicals, media, buffer

Product	Manufacturer
10-beta Competent E. coli	New England Biolabs
2-log DNA ladder	New England Biolabs
Agarose	Carl Roth
AgeI-HF	New England Biolabs
Ampicillin	Carl Roth
Beriglobin	Pharmacy
Bovine serum albumin (BSA)	Santa cruz
BsiWI-HF	New England Biolabs
CruzFluor 488 succumidyl	Santa cruz
Cut Smart Buffer	New England Biolabs
Dimethylsulfoxid (DMSO)	Omnilab
Dulbecco's Modified Eagle Medium (DMEM) Glutamax ™	Gibco™
deoxyribonucleotide triphosphate (dNTP) mix	Invitrogen
Dithiothreitol (DTT)	Carl Roth
Fetal calf serum (FCS)	Biochrom
Fluoroshield™	Sigma-Aldrich
GelRed®	Biotium
Glycerol	Carl Roth
HotStar Taq Plus	Qiagen
Igepal ® CA-630	Sigma-Aldrich
Immu-Mount	Thermo Scientific™
Lysogeny Broth Medium	Carl Roth
Normal goat serum (NGS)	Abcam
Nutridoma™-SP	Roche
Orange G	Sigma-Aldrich
PBS 1x	Gibco™
PCR Buffer	Qiagen
PCR Buffer	High Fidelity Precisor Pol
PEI	Sigma-Aldrich
PFA	Sigma-Aldrich
Primer	Eurofins
Random Hexamer Primer (RHP)	Roche
RNAsin	Promega
RPMI 1640 Medium	Gibco™
SalI-HF	New England Biolabs
SOC	New England Biolabs
SuperScript III	Invitrogen
T4 DNA Ligase	New England Biolabs
Tb Medium	Applichem
XhoI	New England Biolabs

2.2 CSF Samples

In order to perform monoclonal antibody repertoire analysis from patients with different autoimmune encephalitis entities, we established a biobank of CSF samples. We collected seven to 14 ml of CSF from each patient with autoimmune encephalitis either in its acute state or in remission who required lumbar puncture for diagnostic reasons. CSF samples were kept on ice and immediately brought to our facilities, and then centrifuged for ten minutes at 400g at 4°C in order to isolate the cells contained in the sample. Cell pellets were resuspended with 0.5 ml of freezing medium containing 45% FCS, 45% RPMI and 10% DMSO. Resuspended cells were transferred to -80°C. For long term storage, cells were kept in liquid nitrogen until single cell sorting.

2.3 FACS

2.3.1 Single Cell Sorting

We isolated cells of interest from the stored CSF cell pellets into multi-well plates using fluorescence-activated cell sorting. On the day of cell sorting, a lysis solution containing PBS (0.5 x), RNAsin (2 U/µl) and DTT (10 mM) was prepared and transferred to 96-well plates with 4 µl per well. Plates were sealed and kept on ice until FACS sorting. Cells were stained for surface proteins and gating was carried out as described below. Sorted single cell lysates were frozen on dry ice and transferred to storage at -80°C until further processing.

2.3.2 Cell Staining

As preparation for staining, samples were thawed and diluted immediately in 12 ml of sterile FACS Buffer (PBS containing 2% FCS). Centrifugation was performed at 2000g and 4°C for five minutes to separate cells from supernatant. To avoid unspecific binding of antibodies to Fc-receptors expressed by different cell types potentially present among the CSF cells, we performed an Fc-block by resuspending the cells in FACS Buffer containing 1% Beriglobin. This blocking was incubated on ice for ten minutes. A staining solution based on FACS Buffer containing fluorophore-coupled antibodies in concentrations as indicated in table 7 was prepared. After we added 50 µl of antibody solution, cells were incubated for 20 minutes on

ice. We did not wash or filter the samples as the number of cells is the most limiting factor when working with CSF samples. After 20 minutes of incubation with antibody solution, cells were further diluted with FACS Buffer to a total volume of 500 µl. The viability marker DAPI was added right before cell sorting in a final concentration of 1:100.000.

Table 7: Antibody concentrations for FACS staining

Antibody	Fluorophore	Concentration
Anti-CD3	FITC	1:25
Anti-CD14	FITC	1:25
Anti-CD16	Alexa Fluor 488	1:25
Anti-CD20	PerCP-700	1:50
Anti-CD27	APC-Vio770	1:12.5
Anti-CD138	PE	1:50

2.3.3 Gating Strategy

CSF cell samples from patients with autoimmune encephalitis are limited and antibody-secreting cells and B cell populations vary between patients. We therefore used peripheral blood mononuclear cell samples from healthy donors to establish our FACS gating strategy as well as to validate reactivity of antibodies and to derive our compensation matrix. Cell populations of interest were ASC, MBC and nMBC. The following gating strategy was applied: dead cells were identified by penetration of DAPI and excluded from sorting. By relating height (fsc-h) and area (fsc-a) of all events according to their forward scatter, we made sure to take into account only single cells. Lymphocytes were identified by granularity (ssc-a) and size (fsc-a). ASCs are bigger and more granular than average lymphocytes; however, due to their small number, they do not appear as a separate population in FSC/SSC gating. Staining with antibodies targeting CD3, CD14 and CD16 allowed exclusion of T cells, monocytes and natural killer cells. Events positive for CD138 were collected as antibody-secreting cells. Events positive for CD20 were sorted as B cells, with CD27 positive memory B cells being differentiated from CD27 negative non-memory B cells. Generally, all gates were set rather broadly to increase the yield of sorted single cells accepting a higher rate of false-positive sorted events.

2.4 Gene Amplification

To amplify the genes encoding for secreted or membrane-bound antibodies of the sorted cells, we transcribed the mRNA into DNA and subsequently carried out a PCR strategy with separate amplifications for heavy chain, kappa chain and lambda chain for each event.

2.4.1 Reverse Transcription

To make best use of the small amount of mRNA available as a template, reverse transcription was performed directly in the plate into which cells had been sorted. Annealing of random hexamer primers was enabled at 68°C for one minute before the reagents for reverse transcription were added (Tables 8, 9). Polymerization was enabled at 42°C for five minutes and at 25°C for ten minutes, followed by one hour of elongation at 50°C. Enzymes were inactivated at 94°C for five minutes.

Table 8: RHP annealing

Component	Specification	Volume in µl per well
Nuclease free water		2.35
Random Hexamer Primer	300 ng/µl solution	0.50
Igepal CA-630	10% solution	0.50
RNAsin	40 U/µl	0.15
Template	Sorted cell in lysis solution	4.50
Total		8.00

Table 9: Reaction mixture for reverse transcription

Component	Specification	Volume in µl per well
Nuclease free water		2.05
RT Buffer	5x first-strand buffer	3.00
DTT	100 mM	1.00
dNTP Mix	25 mM of each nucleotide	0.50
RNAsin	40 U/µl	0.20
SuperScript III	200 U/µl	0.25
Template	Product of RHP annealing	8.00
Total		15.00

2.4.2 PCR

CDNA produced during reverse transcription was split up into three pathways for amplification of heavy chain, kappa chain and lambda chain:

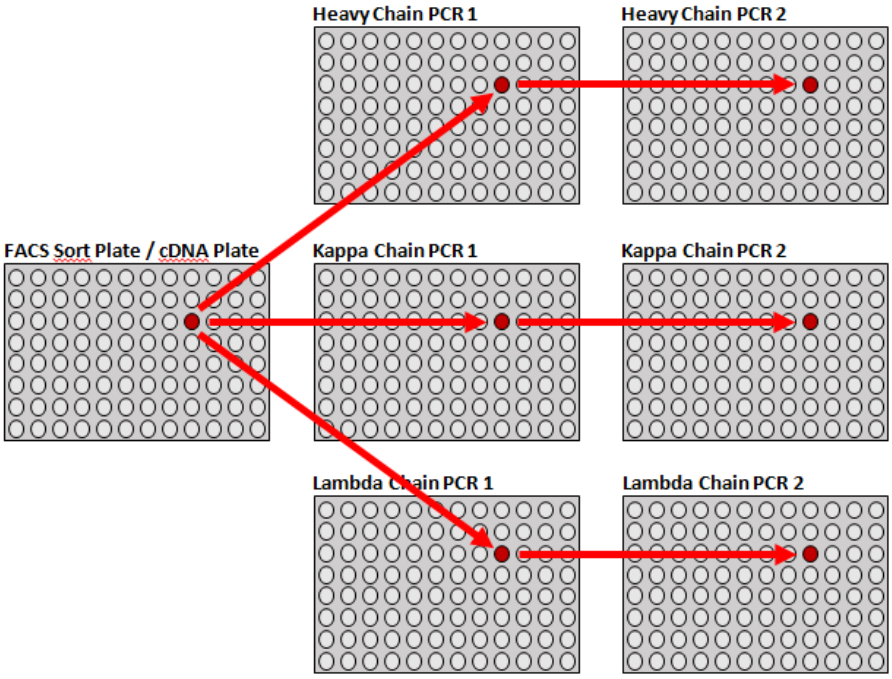

Figure 3: Separate amplification of chain types

To avoid unspecific amplification we chose a two-step nested PCR strategy. 3 µl of cDNA were transferred to a new 96-well plate equipped with master mix for PCR 1 (Table 10) for heavy, kappa and lambda chain, respectively. After an initial step of denaturation (94°C, 15 minutes) we started 50 cycles including the following steps each: denaturation at 94°C for 30 seconds, annealing at 58°C for heavy chains and kappa chains or at 60°C for lambda chains for 30 seconds and elongation at 72°C for 55 seconds. For the last cycle, elongation was extended by ten minutes. PCR 2 was conducted similarly except for the use of 3.5 µl of product derived from PCR 1 as a template and an elongation phase reduced to 45 seconds (Table 11). Master mix without addition of any template served as a negative control. Primer mixes contained primers as indicated in Table 12.

Table 10: Reaction mixture for PCR 1

Component	Specification	Volume in µl per well
Nuclease free water		32.16
PCR Buffer	10x QIAGEN PCR Buffer	4.00
Forward Primer Mix	50 µM combined	0.13
Reversed Primer Mix	50 µM combined	0.13
dNTP Mix	25 mM of each nucleotide	0.40
HotStar Taq	5 U/µl	0.18
Template	cDNA	3.00
Total		40.00

Table 11: Reaction mixture for PCR 2

Component	Specification	Volume in µl per well
Nuclease free water		31.66
PCR Buffer	10x QIAGEN PCR Buffer	4.00
5' Primer Mix	50 µM combined	0.13
3' Primer Mix	50 µM combined	0.13
dNTP Mix	25 mM of each nucleotide	0.40
HotStar Taq	5 U/µl	0.18
Template	Product of PCR 1	3.50
Total		40.00

Table 12: Primers contained in primer mixes for PCR 1 and PCR 2

Primer	Sequence 5‘->3‘
Forward primer mix for heavy chain PCR 1	
H5 1-1	ACAGGTGCCCACTCCCAGGTGCAG
H5 1-2	AAGGTGTCCAGTGTGARGTGCAG
H5 1-3	CCCAGATGGGTCCTGTCCCAGGTGCAG
H5 1-4	CAAGGAGTCTGTTCCGAGGTGCAG
Reversed primer mix for heavy chain PCR 1	
H3 1-1	GGAAGGAAGTCCTGTGCGAGGC
H3 1-2	GGAAGGTGTGCACGCCGCTGGTC
H3 1-3	TGGGAAGTTTCTGGCGGTCACG
Forward primer mix for heavy chain PCR 2	
H5 2/3-1	CTGCAACCGGTGTACATTCCCAGGTGCAGCTGGTGCAG
H5 2/3-2	CTGCAACCGGTGTACATTCCGAGGTGCAGCTGGTGCAG
H5 2/3-3	CTGCAACCGGTGTACATTCTGAGGTGCAGCTGGTGGAG
H5 2/3-4	CTGCAACCGGTGTACATTCTGAGGTGCAGCTGTTGGAG
H5 2/3-5	CTGCAACCGGTGTACATTCCCAGGTGCAGCTGCAGGAG
H5 2/3-6	CTGCAACCGGTGTACATTCCCAGGTGCAGCTACAGCAGTG
Reversed primer mix for heavy chain PCR 2	
H3 2-1	GGGAATTCTCACAGGAGACGA
H3 2/4-2	GTTCGGGGAAGTAGTCCTTGAC
H3 2-3	GTCCGCTTTCGCTCCAGGTCACACT
Forward primer mix for kappa chain PCR 1	
K5 1-1	ATGAGGSTCCCYGCTCAGCTGCTGG
K5 1-2	CTCTTCCTCCTGCTACTCTGGCTCCCAG
K5 1-3	ATTTCTCTGTTGCTCTGGATCTCTG
Reversed primer mix for kappa chain PCR 1	
K3 1	GTTTCTCGTAGTCTGCTTTGCTCA
Forward primer mix for kappa chain PCR 2	
K5 2	ATGACCCAGWCTCCABYCWCCCTG
Reversed primer mix for kappa chain PCR 2	
K3 2/4	GTGCTGTCCTTGCTGTCCTGCT
Forward primer mix for lambda chain PCR 1	
L5 1-1	GGTCCTGGGCCCAGTCTGTGCTG
L5 1-2	GGTCCTGGGCCCAGTCTGCCCTG
L5 1-3	GCTCTGTGACCTCCTATGAGCTG
L5 1-4	GGTCTCTCTCSCAGCYTGTGCTG
L5 1-5	GTTCTTGGGCCAATTTTATGCTG
L5 1-6	GGTCCAATTCYCAGGCTGTGGTG
L5 1-7	GAGTGGATTCTCAGACTGTGGTG
Reversed primer mix for lambda chain PCR 1	
L3 1/4	CACCAGTGTGGCCTTGTTGGCTTG
Forward primer mix for lambda chain PCR 2	
L5 2/3-1	CTGCTACCGGTTCCTGGGCCCAGTCTGTGCTGACKCAG
L5 2/3-2	CTGCTACCGGTTCCTGGGCCCAGTCTGCCCTGACTCAG
L5 2/3-3	CTGCTACCGGTTCTGTGACCTCCTATGAGCTGACWCAG
L5 2/3-4	CTGCTACCGGTTCTCTCTCSCAGCYTGTGCTGACTCA
L5 2/3-5	CTGCTACCGGTTCTTGGGCCAATTTTATGCTGACTCAG
L5 2/3-6	CTGCTACCGGTTCCAATTCYCAGRCTGTGGTGACYCAG
Reversed primer mix for lambda chain PCR 2	
L3 2/3	CTCCTCACTCGAGGGYGGGAACAGAGTG

2.4.3 Gel Electrophoresis

To evaluate gene amplification, gel electrophoresis was performed for every chain type of every event. DNA was marked with GelRed (1:1200) before loading of the gel using Orange G (1:8) as a loading dye. Electrophoresis was performed at 120V for 30 minutes in a TAE gel with 1% agarose. Expected bands for successful amplification were 450 bp (heavy chain), 510 bp (kappa chain) and 405 bp (lambda chain), respectively, referring to a 2-log DNA ladder. For single cell DNA samples from which both a heavy chain and a light chain could be amplified, sequencing followed directly. Detection of either a heavy chain without corresponding light chain or detection of a light chain without corresponding heavy chain led to a single repetition of PCR 1 and PCR 2 of the missing chain type. Samples for which either no light chain or no heavy chain or no chain at all could be amplified were abandoned.

2.5 Sequencing

For positive events where both a heavy and a light chain had been amplified, the product of PCR 2 was sequenced using the corresponding reversed primer used in PCR 2. If quality of sequencing at GATC Eurofins (LightRun) was insufficient for analysis (quality value < 30), we repeated sequencing. Using the IgBlast tool (National Center for Biotechnology Information), we ensured functionality and absence of stop codons, determined the best germline matches for V, D and J gene segments, extracted the sequence of the CDR3 region and noted the number of somatic hypermutations for each amplified immunoglobulin gene. Sequences were searched for sites fitting restriction enzymes that are used in the further course of cloning (AgeI-HF. XhoI. BsiWI-HF, SalI-HF) to avoid digest of DNA at positions other than the ones introduced by our primers. For each gene the immunoglobulin subclass was determined by comparing sequences to the database of the international ImmunoGeneTics information system (Lefranc et al., 2009; Giudicelli et al., 2005). Collecting this information for all events, we checked all amplified genes for clonal relation or identity. We proceeded to cloning if both a heavy chain and at least one light chain had been amplified and were productive according to sequencing results. If several events were entirely identical in their sequence for both heavy and light chains, only one event was pursued.

2.6 Cloning of Monoclonal Antibodies

2.6.1 Specific PCRs

Products retrieved from PCR 1 were purified using the Macherey-Nagel kit for PCR clean-up and gel extraction referring to the manufacturer's user manual NucleoSpin® Gel and PCR clean-up except for predilution of Buffer A1 (1:10) and elution in water (Macherey-Nagel, 2017). Specific PCRs were carried out with primers individually assigned to each chain type of each event. Primers are displayed in Table 14. Restriction sites were introduced with primers to enable cloning (Table 15). 3.5 µl of product of PCR 1 served as template. Temperatures and times applied were the same as for PCR 2 (annealing temperature 58°C). The success of specific PCRs was evaluated by gel electrophoresis (1% agarose in TAE, 120V, 30 min.).

Table 13: Reaction mixture for specific PCRs

Component	Specification	Volume in µl per well
nuclease free water		27.92
PCR Buffer	10x QIAGEN PCR Buffer	4.00
dNTP Mix	25 mM of each nucleotide	0.40
HotStar Taq	5 U/µl	0.18
5' specific Primer	3.3 µM	2.00
3' specific Primer	3.3 µM	2.00
Template	Product of PCR 1	3.50
Total		40.00

Table 14: Primers used for specific PCRs

Primer	Sequence 5‘->3‘
Heavy primers forward	
H5 2/3-1	CTGCAACCGGTGTACATTCCCAGGTGCAGCTGGTGCAG
H5 3-7	CTGCAACCGGTGTACATTCCCAGGTTCAGCTGGTGCAG
H5 3-8	CTGCAACCGGTGTACATTCCCAGGTCCAGCTGGTACAG
H5 2/3-2	CTGCAACCGGTGTACATTCCGAGGTGCAGCTGGTGCAG
H5 2/3-3	CTGCAACCGGTGTACATTCTGAGGTGCAGCTGGTGGAG
H5 3-9	CTGCAACCGGTGTACATTCTGAAGTGCAGCTGGTGGAG
H5 2/3-4	CTGCAACCGGTGTACATTCTGAGGTGCAGCTGTTGGAG
H5 3-10	CTGCAACCGGTGTACATTCTCAGGTGCAGCTGGTGGAG
H5 2/3-5	CTGCAACCGGTGTACATTCCCAGGTGCAGCTGCAGGAG
H5 2/3-6	CTGCAACCGGTGTACATTCCCAGGTGCAGCTACAGCAGTG
H5 3-11	CTGCAACCGGTGTACATTCCCAGCTGCAGCTGCAGGAG
H5 3-12	CTGCAACCGGTGTACATTCCCAGGTACAGCTGCAGCAG
H5 3-13	CTGCAACCGGTGTACATTCTCAGGTGCAGCTGGTGCAATCTGG
Heavy primers reversed	
H3 3-1	TGCGAAGTCGACGCTGAGGAGACGGTGACCAG
H3 3-2	TGCGAAGTCGACGCTGAAGAGACGGTGACCATTG
H3 3-3	TGCGAAGTCGACGCTGAGGAGACGGTGACCGTG
Kappa primers forward	
K5 3-1	CTGCAACCGGTGTACATTCTGACATCCAGATGACCCAGTC
K5 3-2	TTGTGCTGCAACCGGTGTACATTCAGACATCCAGTTGACCCAGTCT
K5 3-3	CTGCAACCGGTGTACATTGTGCCATCCGGATGACCCAGTC
K5 3-4	CTGCAACCGGTGTACATGGGGATATTGTGATGACCCAGAC
K5 3-5	CTGCAACCGGTGTACATGGGGATATTGTGATGACTCAGTC
K5 3-6	CTGCAACCGGTGTACATGGGGATGTTGTGATGACTCAGTC
K5 3-7	TTGTGCTGCAACCGGTGTACATTCAGAAATTGTGTTGACACAGTC
K5 3-8	CTGCAACCGGTGTACATTCAGAAATAGTGATGACGCAGTC
K5 3-9	TTGTGCTGCAACCGGTGTACATTCAGAAATTGTGTTGACGCAGTCT
K5 3-10	CTGCAACCGGTGTACATTCGGACATCGTGATGACCCAGTC
Kappa primers reversed	
K3 3-1	GCCACCGTACGTTTGATYTCCACCTTGGTC
K3 3-2	GCCACCGTACGTTTGATCTCCAGCTTGGTC
K3 3-3	GCCACCGTACGTTTGATATCCACTTTGGTC
K3 3-4	GCCACCGTACGTTTAATCTCCAGTCGTGTC
Lambda primers forward	
L5 2/3-1	CTGCTACCGGTTCCTGGGCCCAGTCTGTGCTGACKCAG
L5 2/3-2	CTGCTACCGGTTCCTGGGCCCAGTCTGCCCTGACTCAG
L5 2/3-3	CTGCTACCGGTTCTGTGACCTCCTATGAGCTGACWCAG
L5 2/3-4	CTGCTACCGGTTCTCTCTCSCAGCYTGTGCTGACTCA
L5 2/3-5	CTGCTACCGGTTCTTGGGCCAATTTTATGCTGACTCAG
L5 2/3-6	CTGCTACCGGTTCCAATTCYCAGRCTGTGGTGACYCAG
Lambda primers reversed	
L3 2/3	CTCCTCACTCGAGGGYGGGAACAGAGTG

2.6.2 Enzymatic Digest

2.6.2.1 Samples

Products of specific PCRs were purified using the Macherey & Nagel PCR Clean-Up Kit as before, starting with 35 µl of PCR product. DNA content was confirmed using UV spectrophotometry. For DNA fragments that contained only the restriction sites brought in by primers, digestion was performed at 37°C for 2 hours, followed by a 20-minute heat shock at 65°C to inactivate added restriction enzymes. Sequences coincidentally containing additional attack points matching our restriction enzymes were exposed to the digestion reaction for only one minute before heat shock. Concentrations of corresponding enzymes were reduced by a factor of ten to avoid full digestion. To evaluate the success of enzymatic digestion, we had a control batch for each enzyme: a vulnerable vector was exposed to the enzyme under the same conditions as our samples and linearization of the vector afterwards was confirmed with gel electrophoresis (1% agarose in TAE, 120V, 40 minutes).

Table 15: Restriction sites for enzymatic digest of samples

	Restriction site 5‘		Restriction site 3‘	
Chain type	**Enzyme**	**Sequence**	**Enzyme**	**Sequence**
Heavy	AgeI-HF	ACCGGT	SalI-HF	GTCGAC
Kappa	AgeI-HF	ACCGGT	BsiWI-HF	CTGACG
Lambda	AgeI-HF	ACCGGT	XhoI	CTCGAG

Table 16: Reaction mixture for enzymatic digest of samples

Component	**Specification**	**Volume in µl per well**
Nuclease free water		4.40
CutSmart Buffer	10x	0.50
AgeI-HF	20 U/µl	0.05
SalI-HF/BsiWI-HF/xhoI	20 U/µl	0.05
Product of specific PCR	purified	5.00
Total		10.00

2.6.2.2 Vectors

Vectors for IGHG1, IGK and IGL contained constant IgG regions, a CMV promotor, an ampicillin resistance and the restriction sites listed below (Wardemann et al., 2003). All vectors were digested in a sequential manner, meaning that only one restriction enzyme at a time was

brought to react. This approach was chosen due to the adjacent restriction sites within the vectors which may lead to interactions between the enzymes if applied at the same time. To ensure extensive digestion, we used 20 U of each enzyme for 1 µg of plasmid DNA. Digestion was performed at 37°C for two hours, followed by a 20-minute heat kill of the enzyme at 65°C. Linearization was assessed using gel electrophoresis after each reaction (1% agarose in TAE, 120V, 40 minutes). To avoid carry-over of undigested vector, DNA was purified from gel using the Macherey & Nagel PCR clean-up gel extraction kit and eluted in water. Concentration and purity of DNA were determined using UV spectrophotometry as before.

Table 17: Restriction sites for enzymatic digest of vectors

	Restriction site 5‘		Restriction site 3‘	
Chain type	**Enzyme**	**Sequence**	**Enzyme**	**Sequence**
Heavy	SalI-HF	GTCGAC	AgeI-HF	ACCGGT
Kappa	BsiWI-HF	CTGACG	AgeI-HF	ACCGGT
Lambda	XhoI	CTCGAG	AgeI-HF	ACCGGT

Table 18: Reaction mixture for enzymatic digest of vectors

Component	**Specification**	**Volume in µl per well**
Vector DNA	1µg/µl	1.00
Nuclease free water		43.00
CutSmart Buffer	10x	5.00
Restriction enzyme (AgeI-HF or SalI-HF or BsiWI-HF or XhoI)	20 U/µl	1.00
Total		50

2.6.3 Ligation

Digested samples were purified and eluted in water. DNA concentration and purity was determined by UV spectrophotometry as before. The required ratio of insert to vector was 3:1 and calculated as follows:

$$\text{insert mass [ng]} = 3 \times \frac{\text{insert length [bp]}}{\text{vector length [bp]}} \times \text{vector mass [ng]}$$

The DNA lengths used for this calculation were heavy chain insert 450 bp, heavy chain vector 5750 bp, kappa chain insert 510 bp, kappa chain vector 5000 bp, lambda chain insert 405bp and lambda chain vector 5000 bp. Each ligation was performed in a 10 µl reaction using 25ng of

vector. Pre-dilutions of samples were calculated to maintain the desired ratio. Ligation was performed for two hours at room temperature. As negative controls we pursued a reaction without insert for each chain type. Moreover, we pursued reactions without vectors as their successful transformation further down the line could indicate contamination in ligation as a linear DNA construct cannot be processed by DH10B competent cells.

Table 19: Exemplary reaction mixture for ligation

Component	Specification	Volume in µl
Insert (heavy chain)	Approx. 0.73 ng/µl	8.00
Vector (heavy chain)	50 ng/µl	0.50
T4 DNA Ligase Buffer	10x	1.00
T4 DNA Ligase	400 U/µl	0.50

2.6.4 Transformation

Ligation product was transformed into DH10B competent cells. For this purpose, competent cells were thawed on ice for two minutes. For each reaction we carefully added 6 µl of competent cells to 2.5 µl of ligation product. The reaction plate was sealed and kept on ice for 30 minutes. After that membrane fluidity was altered by applying a temperature of 42°C for exactly 30 seconds to allow the plasmid DNA to enter the bacterial cells. After incubation on ice for 5 minutes, 100 µl of outgrowth medium (SOC, no antibiotic) was added into each well. Competent cells were then kept at 37°C in SOC medium for 60 minutes. 50 µl each were spread onto selection plates that had been previously prepared with LB agar and ampicillin and had been pre-warmed to 37°C. Bacterial growth was allowed at 37°C overnight. Besides carrying forward the negative controls from ligation, we always incubated one plate with DH10B competent cells without adding DNA to detect contamination.

2.6.5 Insert Check PCRs

We prepared a 96-well PCR plate with master mix for insert check PCRs. Concurrently we set up a 96-well culture plate with 1 ml of TB medium containing 75µg/ml of ampicillin in each well. Each time after picking a colony, we first dipped the pipette tip into a well with master mix and then started the corresponding culture in the culture plate by dropping the tip. In this manner we picked two colonies for each clone. The same primer was used for all insert check

PCRs (Table 20). After running an insert check PCR, we analyzed the PCR products for successful amplification of inserts via gel electrophoresis (1% agarose in TAE, 120V, 40 minutes). Bands at 650 bp for heavy chains, at 700 bp for kappa chains and at 590 bp for lambda chains were evaluated as plasmids containing inserts while bands appearing at 300-400 bp were rated as empty religated vectors.

Table 20: Primer used for insert check PCRs and plasmid sequencing

Primer	Sequence 5‘->3‘
HKL5 4	GCTTCGTTAGAACGCGGCTAC

2.6.6 TB Cultures

For colonies positive in insert check PCRs we inoculated a 4 ml of TB-ampicillin culture for incubation for 37°C for 16-20 hours at 300rpm. Of these cultures we used 0.3 ml to create a glycerol stock for long-term storage by adding 0.3 ml of 40% glycerol solution and instantly cooling it to -80°C. The remaining shares of the cultures were centrifuged to create bacteria pellets (8000 g, 4°C, five minutes).

2.6.7 Plasmid Preparation

DNA was isolated from DH10B competent cells using the Macherey-Nagel NucleoSpin Plasmid QuickPure™ Kit. Bacteria pellets were prepared by resuspension in Buffer A1 (250 µl). Plasmid DNA was liberated from E.coli with supplied SDS/alkaline Buffer A2 (250 µl). Lysates were inverted and kept at room temperature for five minutes. Addition of Buffer A3 (300 µl) created appropriate conditions for the subsequent binding of plasmid DNA. Neutralization was indicated by loss of color. Lysates were cleared from precipitated protein, genomic DNA and cell debris by centrifugation (11,000g, room temperature, ten minutes). Supernatants were centrifuged in NucleoSpin® Plasmid QuickPure Columns to bind DNA (11,000g, room temperature, one minute) and bound DNA was washed with AQ containing ethanol (11,000g, room temperature, three minutes). We dried the silica membrane by centrifugation (11,000g, room temperature, three minutes). For elution, we incubated the columns with pre-warmed H_2O (75 µl, 70°C) for one minute and centrifuged the columns (11,000g, room temperature, one minute). DNA concentrations and purity were determined by

UV spectrophotometry as before. For in-depth testing larger amounts of plasmid were produced using Macherey-Nagel kit for NucleoBond® Xtra maxi plasmid purification. We did this carrying out the manufacturer's protocol for high-copy plasmid purification (Macherey-Nagel, 2014).

2.6.8 Plasmid Sequencing

To ensure no mutations had occurred during the cloning process compared to products of PCR 2, we sent the plasmids in for sequencing using the same primer as for insert check PCRs (Table 20). Sequences were examined using IgBLAST (National Center for Biotechnology Information) and results compared to corresponding sequences of PCR 2. To be approved, chain type, VDJ arrangement and mutation pattern had to be identical. Newly occurring mutations were tolerated if silent. Mutations within the primer binding sites that were in line with return to germline configuration were tolerated as the most probable cause for these mutations was the annealing of our primers. As first sequencing was performed on products of PCR 2 while cloning was done on products of PCR 1, differences between sequence 1 and sequence 2 could also have originated in PCR 2 and therefore be irrelevant for cloning. For sequencing results of numerous colonies that were identical to each other but differing from sequence 1, we assumed irrelevant mutations in PCR 2 to be the most probable cause for discrepancy. Corresponding plasmids were thus processed further. The presence of unacceptable mutations resulted in picking new colonies until a correct plasmid was identified. If more than five colonies did not contain a satisfactory plasmid, cloning was evaluated as not successful and repeated.

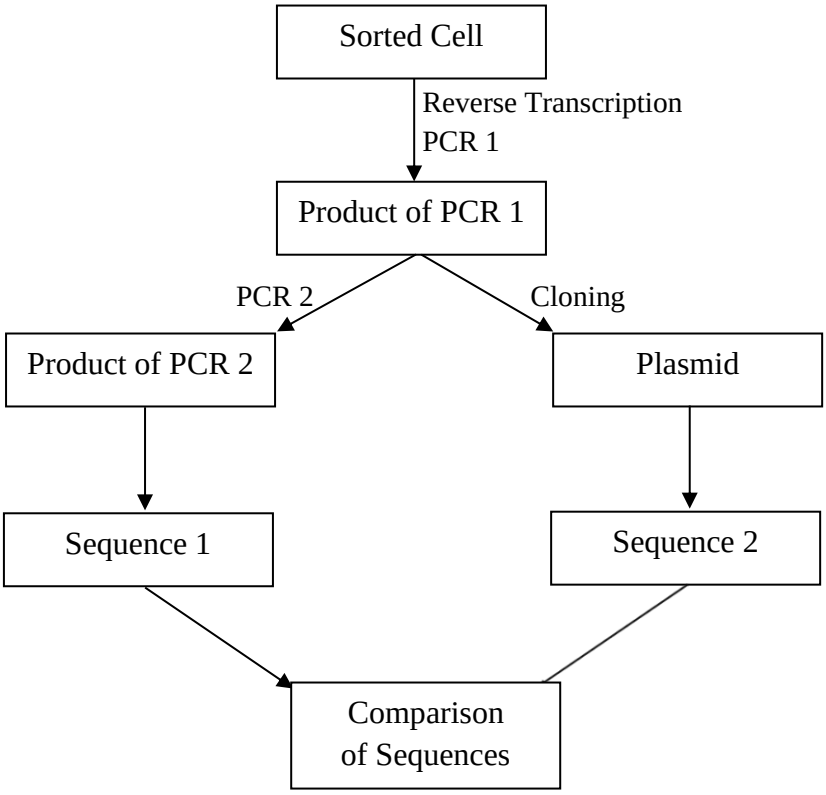

Figure 4: Origin of sequences for analysis and comparison

2.7 Expression in HEK cells

2.7.1 Transfection

When plasmids encoding both for heavy and for light chain of an event were available, they were co-transfected in HEK cells. Cells were cultivated in DMEM containing 5.5% GlutaMAX™, 10% FBS, 100µg/ml of streptomycin and 100 U/ml of penicillin. Cells were split one day prior to transfection with a required cell density of 50-70% at the time of transfection. Right before transfection, medium was changed to DMEM containing 1% Nutridomna-SP. PEI and NaCl were pre-warmed to 37°C and brought together with plasmid DNA. Reaction mixtures were immediately vortexed thoroughly. After 15 minutes of incubation at room temperature, mixtures were applied to the cells (Table 21). Supernatant was harvested after incubation at 37°C and 5% CO_2 for three days. Cell debris was removed by centrifugation (2000g, 4°C, five minutes). Sodium azide was added to all supernatants at a final concentration of 0.05%.

Table 21: Transfection of HEK cells

Receptacle area in cm^2	Nutridoma medium in ml	NaCl in µl	PEI in µl	DNA heavy chain in µg	DNA light chain in µg
9.4	2.0	110	9.5	0.95	0.95
60.0	10.0	700	60.0	6.00	6.00
149.0	25.0	1750	150.0	15.00	15.00

2.7.2 ELISA

Concentrations of monoclonal antibodies in supernatant were determined by ELISA using Mabtech human IgG ELISA and the corresponding manufacturer's protocol (Mabtech, 2013). Each supernatant was measured in eight different dilutions and at two different points in time to calculate concentrations. Linear range for regression was determined manually. Results below 1µg/ml were evaluated as negative and transfections were repeated for corresponding events.

2.8 Screening for Reactivity

For screening, supernatants were applied to brain slices or cells without further processing. Antibodies originating from AI-ENC 136 were purified for in-depth testing by Jakob Kreye (DZNE, Charité). Supernatants were incubated with Protein G Sepharose® beads (4°C, overnight, rotating mixer). Beads were separated from supernatant by centrifugation (4000g, 4°C, ten minutes) and applied to chromatography spin columns and washed with PBS. Antibodies were eluted with sodium citrate (0.1 M, pH 2.7) and neutralized with TRIS Buffer (1 M, pH 8.8). Antibodies were dialyzed against PBS (4°C, overnight).

2.8.1 Immunohistochemistry

Slices cut from unfixed murine brains were used for immunohistochemistry. For some experiments, tissue was fixed either with PFA (room temperatures, ten minutes) or methanol (three minutes, -20°C). PBS-based blocking solution containing 5% NGS, 2% BSA and 0.05% NaN_3 was applied to the tissue sections for one hour. Undiluted supernatants or purified antibodies were incubated on the slices in wet chambers at 4°C overnight. Fluorophore-

conjugated secondary antibodies reactive to human IgG were diluted in blocking solution and put on the sections for two hours at room temperature. The procedure was completed using ImmuMount™ or Fluoroshield™ with DAPI.

2.8.2 Cell-based Assays

To test our monoclonal antibodies against specific epitopes we transfected HEK cells with mGluR5 or Progranulin. Two days after transfection cells were fixed with methanol (-20°C, three minutes) or PFA (room temperature, ten minutes). After incubation with blocking solution (5% NGS, 2% BSA, 0.05% NaN_3) for one hour, supernatant containing monoclonal antibodies was applied to the cells and left overnight (4°C, 50rpm). Secondary antibodies were added and incubated (room temperature, two hours) before completing with Immu-Mount™ or Fluoroshield™ with DAPI.

2.8.3 Fluorescence Microscopy

Stained brain sections and HEK cells were analyzed using fluorescence microscopy to evaluate reactivities of our cloned antibodies. Antibodies known to show no effect on these tissues or blocking solution without antibodies were used as negative controls, while antibodies with known reactivity were used as positive controls. Images were edited with Adobe Illustrator or Adobe Photoshop. If images were modified, all images of one experiment were modified in a comparable way. Scale bars were generated at the microscope or reconstructed afterwards.

2.9 Fab Fragments

2.9.1 Conjugation of Antibodies with Fluorophore

To conjugate monoclonal antibodies with fluorophores, they were rebuffered in carbonate buffer (pH 8.5). CruzFluor 488 succumidyl ester was diluted in DMSO (10 mg/ml). We then incubated 1mg of antibody with 8.4 µl of the fluorophore suspension (1:20) for one hour (room temperature, 200rpm,). Loose molecules of fluorophore were removed by centrifugation

through Amicon Ultra centrifugal filters (cut-off 100 kDa). Eluted antibody concentrates were then analyzed for attached fluorophores using UV spectrophotometry.

2.9.2 Fab Cloning

Fab fragments generally consist of a shortened heavy chain and a full-length light chain connected to each other via disulfide bridges as in full IgG molecules (King, 1998). Therefore, only modification of the heavy chain is necessary for the conversion of a regular antibody into a Fab fragment while the light chain remains unchanged. On a protein level, Fab fragments can be generated by papain digest (Hughes et al., 2010). However, we modified DNA encoding for full IgG to encode for Fab fragments. With the aim to generate Fab fragments with variable regions identical to our monoclonal antibodies, the following strategy was carried out.

2.9.2.1 Fab PCR Strategy

Plasmids encoding for the regular heavy chains of monoclonal antibody HL 003-102 produced and described in our lab previously served as a template. The same forward primer as used for amplifying full IgG of this antibody was also used for Fab cloning (Table 22).

Table 22: Forward primer used for Fab cloning

Heavy chain	Primer Name	Sequence of Forward Primer 5'->3'
003-102	H5 2/3-5	CTGCAACCGGTGTACATTCCCAGGTGCAGCTGCAGGAG

As our experiments were to be based on the findings of Hughes et al. (2010), we created Fab fragments of a comparable size and structure. Therefore, the Fc part of the antibodies had to terminate at the papain restriction site. On a DNA level this was realized by the use of reversed primers annealing to the sequence encoding for the papain restriction site. A FLAG-Tag, a stop and a restriction site for XhoI were introduced into the sequence by reversed primers (Figure 5).

Figure 5: DNA sequence inserted by Fab reversed primers

Aimed DNA sequence to be introduced by reversed primer

5'-AAATCTTGTGACAAAACTCACGACTATAAGGACGACGACGACAAGTGACTCGACCAA-3'
3'-TTTAGAACACTGTTTTGAGTGCTGATATTCCTGCTGCTGCTGTTCACTGAGCTGGTT-5'

■ Annealing to template ■ FLAG-Tag ■ STOP-Codon ■ XhoI restriction site

A reversed primer containing both a binding site long enough for sufficient annealing as well as the required sequences described above would have been too long and therefore have provided unfavorable binding characteristics such as a high melting temperature. For this reason the desired sequence was introduced by two overlapping primers, FLAG 1 and FLAG 2, used in two sequential PCR reactions (Figure 6).

Figure 6: Fab reversed primers

Primer	Sequence 3'-> 5'	Tm
FLAG 0	TTTAGAACACTGTTTTGAGTGCTGATATTCCTGCTGCTGCTGTTCACTGAGCTGGTT	72°C
FLAG 1	TTTAGAACACTGTTTTGAGTGCTGATATTCCTGCTGCT	64°C
FLAG 2	TGCTGATATTCCTGCTGCTGCTGTTCACTGAGCTGGTT	70°C

■ Annealing to template ■ FLAG-Tag ■ STOP-Codon ■ XhoI restriction site

Despite allocation of the sequence to two primers, the annealing of the long reversed primers to the template was expected to be error-prone. We therefore elected Precisor Pol as an enzyme with very low error rates even when dealing with challenging templates and primers. Additionally, the number of cycles was reduced to 25 compared to our regular procedure when cloning full IgG antibodies.

a) Fab PCR 1

The reaction for Fab PCR 1 was set up as shown in Table 23. The plasmid encoding for the full IgG heavy chain 003-102 was used as a template. After an initial step of denaturation (98°C, two minutes), we started 25 cycles including the following steps each: denaturation at 98°C for 30 seconds, annealing at 55°C for 30 seconds and elongation at 72°C for one minute. For the last cycle, elongation was extended by seven minutes. Master Mix without addition of any template served as a negative control. PCR products were cooled to 4°C immediately until further processing.

Table 23: Reaction mixture for Fab PCR 1

Component	Specification	Volume in µl per well
Nuclease free water		32.00
PCR Buffer	5x High Fidelity Buffer	10.00
5' Primer according to heavy chain	10 µM	2.00
3' Primer FLAG 1	10 µM	2.00
dNTP Mix	25 mM of each nucleotide	0.50
PrecisorPol	2 U/µl	1.00
DMSO		1.50
Template (Plasmid heavy chain)	50 ng/µl	1.00
Total		50.00

b) Fab DNA Purification 1

To avoid carry-over of the plasmid used as a template, we purified the product of PCR 1 by gel extraction. To do so, 50 µl of PCR 1 product were loaded into a 1% agarose-TAE gel with GelRed© and Orange G. After gel electrophoresis (120V, 40 minutes), the band located at the expected size of 0.750kb was isolated. Purification was performed using the Macherey & Nagel PCR clean-up gel extraction kit according to the manufacturer's protocol (Macherey-Nagel, 2017). Isolated DNA was diluted in Buffer NE.

c) Fab PCR 2

The reaction for Fab PCR 2 was set up as shown in Table 24 using the product of Fab PCR 1 as a template. Temperatures, times and number of cycles for Fab PCR 2 were identical to the ones used for Fab PCR 1. The product of PCR 2 was purified in the same manner as the product of PCR 1.

Table 24: Reaction mixture for Fab PCR 2

Component	Specification	Volume in µl per well
Nuclease free water		32.00
PCR Buffer	5x High Fidelity Buffer	10.00
5' Primer according to heavy chain	10 µM	2.00
3' Primer FLAG 2	10 µM	2.00
dNTP Mix	25 mM of each nucleotide	0.50
PrecisorPol	2 U/µl	1.00
DMSO		1.50
Template (Product Fab PCR 1)	50 ng/µl	1.00
Total		50.00

d) Fab Enzymatic Digest

Enzymatic digest was conducted at the restriction sites introduced by primers (5': AgeI-HF, 3': XhoI) at 37°C for two hours, followed by inactivation of the enzymes by heat (65°C, 20 minutes). To control functionality of enzymes, a sample containing a vector vulnerable to each enzyme in question was carried along, and its linearization was confirmed with gel electrophoresis (1% agarose in TAE, 120V, 40 min.). After renewed purification, presence and purity of DNA were confirmed using UV spectrophotometry.

Table 25: Enzymatic digest of Fab PCR 2 products

Component	Specification	Volume in µl per well
Nuclease free water		4.40
CutSmart Buffer	10x	0.50
AgeI-HF	20 U/µl	0.05
XhoI	20 U/µl	0.05
Product of specific PCR	purified	5.00
Total		10.00

e) Fab Ligation

Due to altered size of insert compared to cloning of full IgG antibodies, the formula used for cloning of full IgG antibodies was adjusted.

$$\text{insert mass [ng]} = 3 \times \frac{750 \text{ bp}}{5750 \text{ bp}} \times \text{vector mass [ng]}$$

In order to maintain the ratio of insert to vector of 3:1, ligation was conducted in a 10 µl reaction at room temperature for two hours. Besides a negative control containing only vector but no insert, we carried along a negative control lacking vector to exclude presence of the plasmid used as a template for PCRs in insert samples.

Table 26: Ligation of Fab heavy chain

Component	Specification	Volume in µl
Insert (Fab heavy chain)	2.67 ng/µl	7.50
Vector (heavy chain)	50 ng/µl	1.00
T4 DNA Ligase Buffer	10x	1.00
T4 DNA Ligase	400 U/µl	0.50
Total		10.00

2.9.3 Expression of Fab Fragments in HEK Cells

Transformation, preparation of plasmid DNA and transfection of HEK cells were performed as described for cloning of full IgG antibodies (compare chapters 2.6.4 to 2.7.1).

2.9.4 Purification of Fab IgG Antibodies from HEK Cell Supernatant

Three days after co-transfecting HEK cells with Fab heavy chain 003-102 and the regular light chain 003-102, supernatant was harvested. Cell debris was removed by centrifugation (2000g, 4°C, five minutes). Fab fragments were purified with Anti-FLAG M2 Magnetic beads based on the manufacturer's protocol (Sigma-Aldrich, 2013). The pH of the supernatant was adjusted to 7.5. Anti-FLAG M2 beads were washed with TBS twice before adding of the supernatant for incubation on a rotating mixer (4°C, overnight). Beads were collected with a magnetic separator and supernatant was removed. Beads were washed with TBS. Fab fragments were eluted with 0.1M glycine HCl and pH was equilibrated immediately with 1M TRIS Buffer. Fab fragments were concentrated with Amicon filter tubes (cut-off 10 kDa) and eluted in PBS.

3 Results

3.1 Patient Characteristics

Analysis of monoclonal antibody repertoire was carried out for six patients, from whom we had received one CSF sample each. CSF or serum of each of these patients had been shown to react against either mGluR5 or Progranulin. Furthermore, all patients showed symptoms consistent with encephalitis, ranging from severe dysautonomia and altered consciousness to neuropsychiatric disorders such as changes in personality and behavior as well as mnemic and cognitive deficits. Comorbidities were not considered. Cell counts in CSF provided by the laboratories carrying out routine diagnostics ranged from 0 to 21/µl (Table 27).

Table 27: Patient characteristics

Patient ID	Antibody defining autoimmune encephalitis	Age [years]	Gender	CSF cell count [n/µl]
AI-ENC 001	anti-mGluR5 antibodies	30	F	2
AI-ENC 082	anti-mGluR5 antibodies	27	F	1
AI-ENC 136	anti-mGluR5 antibodies	14	M	21
AI-ENC 148	anti-mGluR5 antibodies	34	M	1
AI-ENC 158	anti-Progranulin antibodies	39	F	5
AI-ENC 159	anti-Progranulin antibodies	76	M	0

3.2 Flow Cytometry-based Single Cell Sorting

Out of the six cell pellets, we isolated 405 cells in total using flow cytometry-based single cell sorting, of which 209 originated from patients whose encephalitis was associated with anti-mGluR5 antibodies and 196 from patients in whom encephalitis was associated with antibodies against Progranulin. The number of cells sorted from one sample ranged from 33 to 156, and the distribution of cell types varied among patients (Table 28). For all other samples, the share of antibody-secreting cells expressing CD138 was between 2.65% (AI-ENC 136) and 55.88% (AI-ENC 082). Memory B cells which were CD20 positive as well as CD27 positive made up a share of 2.94% (AI-ENC 082) to 39.39% (AI-ENC 148). Information on cell types of sorted cells of patients AI-ENC 158 and AI-ENC 159 was considered invalid due to the high background signal in ASC channel caused by PE-conjugated anti-CD138 antibody and was therefore not included in this analysis of subpopulations. With a percentage of 64.66% on average, non-memory B cells which were CD20 positive, but CD27 negative made up the biggest portion among all sorted cells, ranging from 41.18% (AI-ENC 082) to 84.07% (AI-ENC 136).

Table 28: Number and type of sorted cells

Patient ID	Autoimmune encephalitis defining autoreactivity	Sorted Cells			
		Total	ASC	MBC	NMBC
AI-ENC 001	anti-mGluR5 autoreactivity	29	4	7	18
AI-ENC 082	anti-mGluR5 autoreactivity	34	19	1	14
AI-ENC 136	anti-mGluR5 autoreactivity	113	3	15	95
AI-ENC 148	anti-mGluR5 autoreactivity	33	6	13	14
AI-ENC 158	anti-Progranulin autoreactivity	156	109	9	38
AI-ENC 159	anti-Progranulin autoreactivity	40	14	6	20

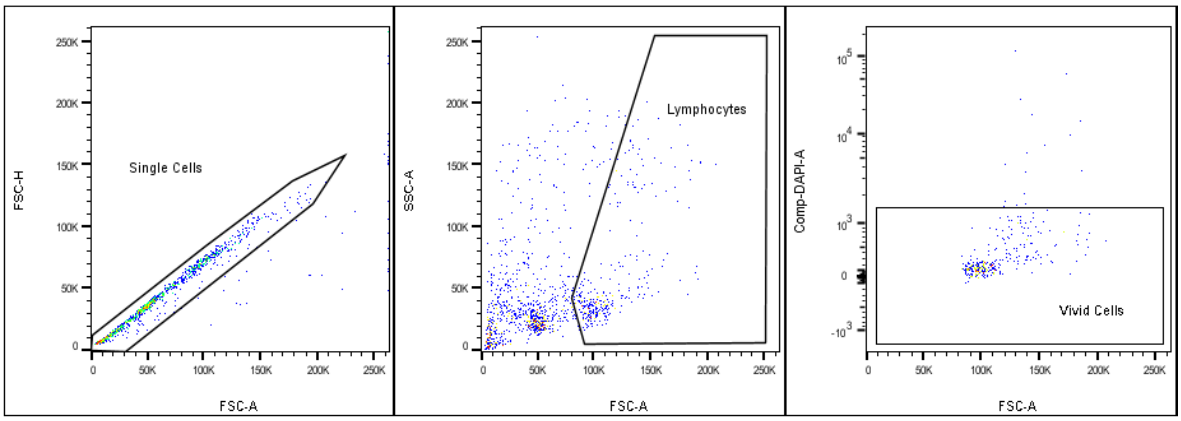

Figure 7: Exemplary gates for preselection of CSF cells. Single cells, lymphocytes and vivid cells were preselected in flow cytometry to isolate cells of interest.

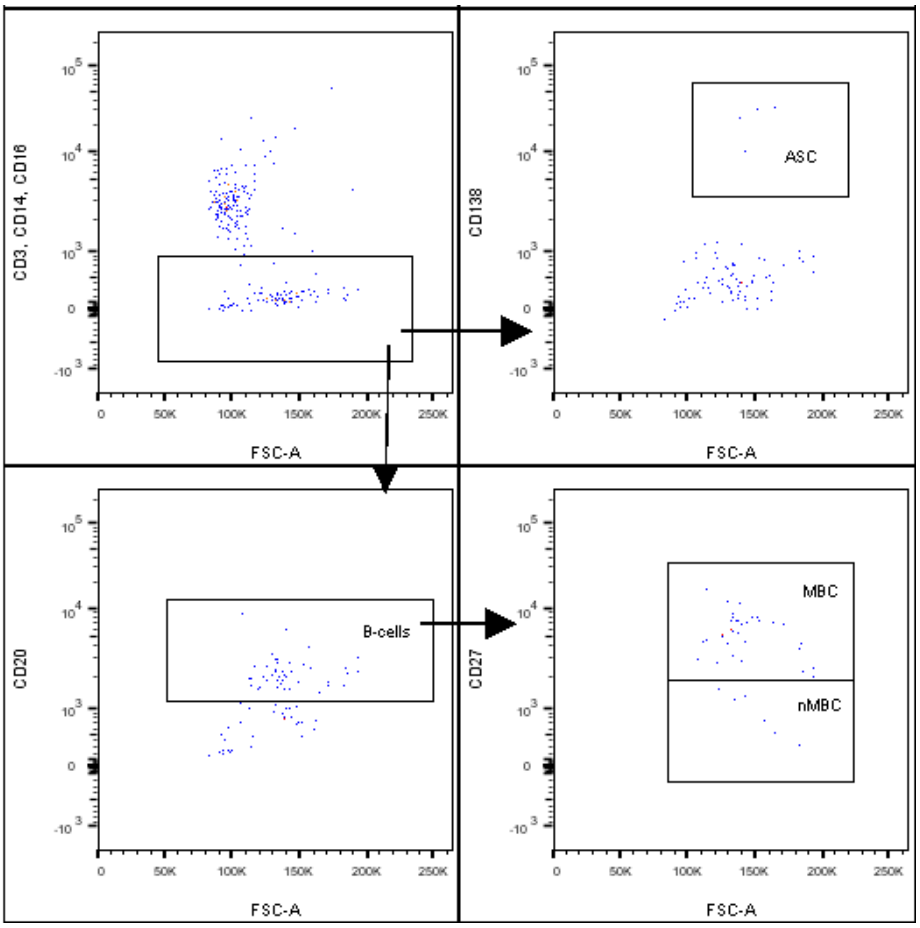

Figure 8: Exemplary gates for selection of ASCs, nMBCs and MBCs out of CSF cells after preselection. Cells that were negative for CD3, CD4 and CD16 but positive for CD138 were sorted as ASCs. Cells that were negative for CD3, CD4 and CD16 but positive for CD20 were sorted as B cells while differentiation was made between CD27 positive MBCs and CD27 negative nMBCs.

3.3 Polymerase Chain Reactions

Aiming to amplify the variable immunoglobulin genes of a heavy chain and light chain of each sorted cell, we achieved varying results. For some, both a heavy chain and a light chain (51 cells) and, for few events, a heavy chain as well as both a kappa and a lambda chain (eight cells) were amplified successfully. Purification and sequencing was performed only on cells for which both a heavy chain and at least one type of light chain were amplified (Figure 10). Cells for which we did not succeed in amplifying any chain type or only one type of chain without a corresponding partner to pair with were no longer pursued. Amplification was confirmed by gel electrophoresis (Figure 9).

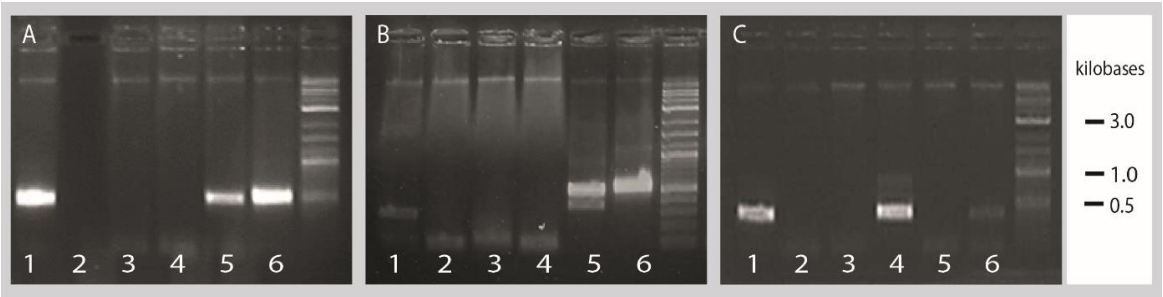

Figure 9: Gel electrophoresis of products of PCR 2 from six exemplary single cell DNA samples. Immunoglobulin chains were amplified separately according to chain type and PCR products were visualized using gel electrophoresis. Successful gene amplicons appear as bands at 0.450 kb for heavy chains (A, lane 1, 5, 6), at 0.510 kb for kappa chains (B, lane 5, 6) and at 0.405 kb for lambda chains (C, lane 1, 4, weak in lane 6).

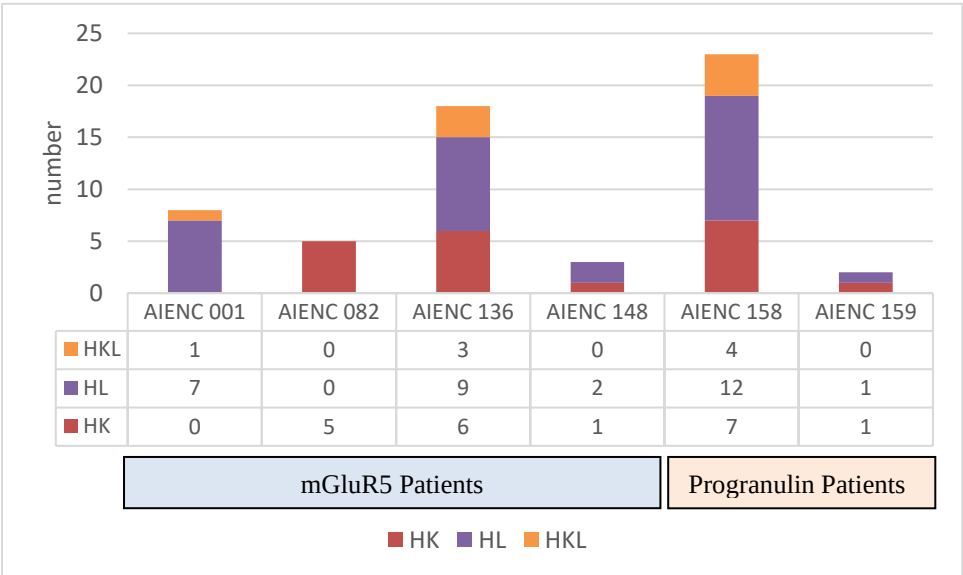

Figure 10: Number of successful amplifications according to chain type and patient. Chain types: heavy (H), kappa (K) and lambda (L).

3.4 Sequencing

For all 59 successfully amplified chain pairs or triplets we carried out sequencing to examine the sequences for immunoglobulin subtypes, gene family usage, number of SHM and clonal relation or identity. Sequencing revealed IgG to represent the biggest fraction of all immunoglobulin classes among the events successfully processed for both the mGluR5 and the Progranulin group. Further analysis of this group showed subclass IgG1 to be the strongest representative with 32 out of 59 events. IgM could be identified as a marker for acute immune response in three out of four patients in the mGluR5 group and in one of two in the Progranulin group (Figure 11). Aligning the sequences of our immunoglobulin chains with germline genes using the IgBlast tool (National Center for Biotechnology Information) allowed identification of the chain segments they originated from for most but not for all chains. None of the sequences matched germline configuration completely in the narrower sense of naturally occurring antibodies, with the number of SHM ranging from 1 to 32. For AI-ENC 82, however, two out of five heavy chains featured only one SHM each. The same was true of one kappa chain retrieved from AI-ENC 001. Screening for clonality among the potential anti-mGluR5 antibodies showed heavy chains of events 136-143 and 136-181 to be made up of identical germline genes for all three segments V, D and J and only differing in their pattern of SHM. Similarly, kappa chains of events HK 136-169 and HK 136-187 originated from identical segments but varied in their SHM. Out of three events successfully amplified for AI-ENC 148, two featured lambda chains with equivalent usage of like segments. Searching for clonal expansion amongst potential anti-Progranulin antibodies led to several findings: heavy chains for ASC 158-123 and ASC 158-242 were identical both regarding gene usage and SHM pattern, though light chains differed. While in ASC 158-123 this heavy chain was paired with a lambda chain containing V segment 2-23, V segment 8-61 was found in ASC 158-242. Both of these V segments reoccurred throughout the antibody repertoire: V segment 2-23 was identified in five lambda chains of AI-ENC 158 overall while none of these immunoglobulins were consistent in their other segments. For two of these events containing V segment 2-23, no other segments could be identified. Similarly, two of the lambda chains of AI-ENC 158 contained V segment 8-61 while neither D nor J segment could be detected. Furthermore, we were able to assign specific primers to each amplified immunoglobulin chain based on these sequencing results to pursue cloning.

Table 29: Sequencing results of mGluR5 patients. Sequences were generated and analyzed after PCR 2 and originate from single cells retrieved from patients with mGluR5 associated autoimmune encephalitis. Change in background color indicates a new patient sample. F = Function, CDR3l = CDR3 length, SHM = Somatic hypermutations, N/A not available, Y = Yes, N = No

ID	Cell	Ig subclass	Chain type	Segment			CDR3l	SHM	F
				V	D	J			
001-103	nMBC	IgM	heavy	3-23	3-22	4	N/A	25	Y
			lambda	2-11		1	10	8	Y
001-106	nMBC	IgG1	heavy	3-23	1-26	4	13	16	Y
			kappa	1-39		2	9	16	Y
			lambda	2-23		1	9	5	Y
001-107	nMBC	IgA1	heavy	1-69	1-26	5	17	32	Y
			lambda	3-1		3	9	1	Y
001-116	MBC	IgG1	heavy	3-53	1-26	4	N/A	31	Y
			lambda	1-44		2	12	14	Y
001-117	nMBC	IgG1	heavy	5-51	3-3	6	20	20	Y
			lambda	2-23		1	26	14	Y
001-118	nMBC	IgA1	heavy	4-39	3-9	4	22	10	Y
			lambda	1-44		3	11	23	Y
001-124	nMBC	IgG1	heavy	4-59	1-7	4	28	23	Y
			lambda	6-57		2	11	27	Y
001-126	MBC	IgM	heavy	4-34	2-21	4	14	11	Y
			lambda	7-43		1	24	16	Y
082-103	nMBC	IgM	heavy	1-18	2-15	3	17	1	Y
			kappa	4-1		1	9	3	Y
082-105	nMBC	IgM	heavy	3-7	5-12	6	20	8	Y
			kappa	3-15		2	9	22	Y
082-113	MBC	IgG1	heavy	4-34	3-10	5	20	9	Y
			kappa	3-20		2	11	7	Y
082-129	nMBC	IgM	heavy	4-4	5-18	2	19	1	Y
			kappa	2-28		4	9	5	Y
082-130	nMBC	IgM	heavy	3-33	5-12	44	15	17	Y
			kappa	3-11		4	9	8	Y
136-103	ASC	IgM	heavy	3-15	3-16	6	22	8	Y
			lambda	2-11		1	8	7	Y
136-105	nMBC	IgM	heavy	3-23	3-22	6	19	15	Y
			lambda	3-1		2	9	20	Y
136-118	nMBC	IgG1	heavy	1-46	3-16	6	14	11	Y
			lambda	2-23		3	10	24	Y
136-119	nMBC	IgG1	heavy	3-74	7-27	4	9	4	Y
			lambda	3-21		3	12	13	Y
136-133	nMBC	IgA1	heavy	3-23	5-12	4	17	15	Y
			kappa	1-5		1	9	10	Y
136-143	ASC	IgG1	heavy	3-11	3-10	2	17	9	Y
			lambda	3-1		2	10	15	Y
136-149	nMBC	IgM	heavy	3-30	5-18	5	17	31	Y
			kappa	3-11		1	9	9	Y

136-161	nMBC	IgG1	heavy	4-59	N/A	6	13	17	Y
			lambda	1-44		3	11	7	Y
136-162	nMBC	IgG1	heavy	3-11	4-17	2	20	9	Y
			kappa	3-20		2	10	4	Y
			lambda	2-23		2	11	51	Y
136-169	nMBC	IgG1	heavy	4-61	1-14	6	15	10	Y
			kappa	3-15		4	8	5	Y
136-170	MBC	IgG1	heavy	4-39	6-19	5	15	12	Y
			kappa	3-15		5	10	8	Y
136-171	nMBC	IgG2	heavy	4-4	3-9	4	6	23	Y
			lambda	2-14		1	10	4	Y
136-180	nMBC	IgG1	heavy	3-7	6-19	6	17	7	Y
			kappa	2-28		2	10	5	Y
			lambda	6-57		2	9	2	Y
136-181	MBC	IgG1	heavy	3-11	3-10	2	17	14	Y
			lambda	2-23		N/A	N/A	12	Y
136-184	nMBC	n/d	heavy	3-48	2-2	4	N/A	N/A	Y
			kappa	1-5		1	8	6	Y
			lambda	2-8		7	17	N/A	Y
136-186	MBC	IgG1	heavy	3-9	6-19	1	16	29	Y
			kappa	3-15		2	N/A	20	Y
136-187	nMBC	IgG1	heavy	4-34	2-15	1	18	6	Y
			kappa	3-15		4	10	6	Y
136-196	nMBC	IgM	heavy	1-8	3-22	5	12	3	Y
			lambda	2-14		1	10	20	Y
148-104	MBC	IgG1	heavy	3-30	2-2	6	21	20	Y
			lambda	1-47		3	12	9	Y
148-111	MBC	IgG3	heavy	4-34	2-21	6	12	10	Y
			lambda	1-47		3	11	22	Y
148-112	MBC	IgG1	heavy	3-33	5-12	4	15	17	Y
			kappa	1-5		1	9	18	Y

Table 30: Sequencing results of Progranulin patients. Sequences were generated and analyzed after PCR 2 and originate from single cells retrieved from patients with Progranulin-associated autoimmune encephalitis. Change in background color indicates a new patient sample.

ID	Cell	Ig subclass	Chain type	Segment			CDR3l	SHM	F
				V	D	J			
158-104	ASC	IgG2	heavy	3-33	2-21	4	9	16	Y
			kappa	3-20		2	9	14	Y
158-107	ASC	IgM	heavy	1-2	3-3	4	13	6	Y
			kappa	3-11		2	9	6	Y
158-108	nMBC	IgG1	heavy	5-10-1	5-12	4	14	10	Y
			kappa	1-27		N/A	N/A	N/A	N
158-110	ASC	IgG4	heavy	4-39	N/A	6	9	15	Y
			lambda	6-57		2	11	8	Y
158-117	nMBC	IgG1	heavy	4-59	N/A	4	10	15	Y

			kappa	2-28		2	9	30	Y
			lambda	2-23		1	10	15	Y
158-123	ASC	IgG1	heavy	3-11	3-10	4	13	19	Y
			lambda	2-23		N/A	N/A	N/A	N
158-126	nMBC	n/d	heavy	3-30	2-2	4	N/A	N/A	N
			kappa	3-20		1	8	15	Y
158-130	ASC	IgG1	heavy	4-39	2-15	4	16	1	Y
			lambda	2-23		N/A	N/A	19	N
158-156	nMBC	IgG1	heavy	1-69	2-8	4	18	7	Y
			lambda	2-14		2	11	7	Y
158-158	nMBC	IgG1	heavy	1-18	3-3	6	17	21	Y
			lambda	2-23		2	11	16	Y
158-178	nMBC	IgG1	heavy	1-18	5-18	4	16	20	Y
			kappa	1-39		1	9	17	Y
158-191	nMBC	IgA1	heavy	3-23	3-10	5	15	20	Y
			kappa	1-39		5	10	17	Y
158-207	nMBC	IgG2	heavy	4-34	2-2	3	N/A	N/A	N
			kappa	3-15		4	9	22	Y
158-211	nMBC	IgG2	heavy	3-53	6-19	5	13	23	Y
			kappa	4-1		4	8	31	Y
			lambda	3-21		3	10	20	Y
158-213	nMBC	IgG1	heavy	1-46	3-16	6	32	25	Y
			lambda	1-40		2	11	22	Y
158-216	nMBC	IgG1	heavy	4-59	2-2	6	22	18	Y
			kappa	1-13		3	9	8	Y
			lambda	3-25		2	11	3	Y
158-231	ASC	IgG1	heavy	4-59	N/A	4	10	14	Y
			lambda	8-61		N/A	N/A	15	N
158-237	nMBC	IgG1	heavy	1-69	6-13	6	22	15	Y
			lambda	2-14		2	11	11	Y
158-239	MBC	IgM	heavy	3-7	2-2	6	20	20	Y
			lambda	1-47		3	12	21	Y
158-241	nMBC	IgA1	heavy	3-64D	7-27	4	12	23	Y
			kappa	1-39		2	9	23	Y
			lambda	3-21		3	11	1	Y
158-242	ASC	IgG1	heavy	3-11	3-10	4	13	19	Y
			lambda	8-61		N/A	N/A	N/A	Y
158-250	nMBC	IgA1	heavy	3-11	1-1	6	18	7	Y
			lambda	2-23		1	9	6	Y
158-251	ASC	IgG1	heavy	1-2	2-8	4	10	13	Y
			lambda	2-8		2	10	13	Y
159-113	MBC	IgG2	heavy	3-74	3-22	6	11	14	Y
			lambda	2-8		1	10	7	Y
159-147	MBC	IgG1	heavy	5-10-1	2-21	4	15	27	Y
			kappa	1-39		2	9	28	Y

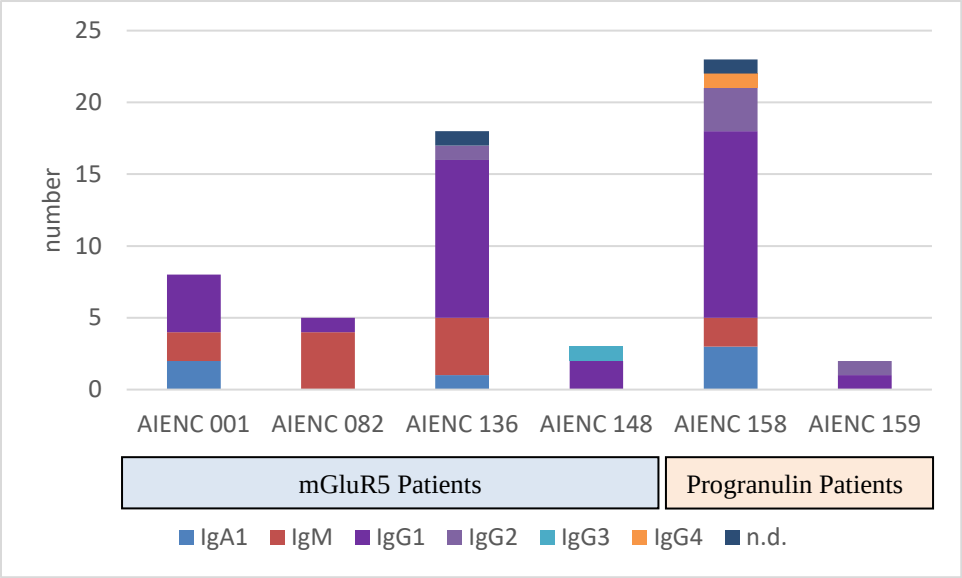

Figure 11: Distribution of immunoglobulin subtypes among patients

3.5 Cloning

Out of all purified and sequenced samples (59 heavy chains, 28 kappa chains, 40 lambda chains), three heavy chains, one kappa chain and three lambda chains including their corresponding chains were abandoned due to lack of productivity of genes as revealed by sequence analysis using the IgBlast tool (National Center for Biotechnology Information). Overall, 56 heavy chains, 27 kappa chains and 37 lambda chains were brought into specific PCRs, of which all but four lambda chains were successfully amplified. All resulting products of specific PCRs were purified and then underwent enzymatic digest. Photospectrometry proved continual presence of DNA in samples after renewed purification. All genes were then ligated into IgG1, IgK and IgL vectors, respectively, and generated plasmid DNA was transformed into E.coli DH10B. Growth of colonies was observed for all events, with negative controls showing no growth. Retrieving DNA from picked colonies as a template, we confirmed the presence of amplified genes in plasmids by an insert check PCR for each chain. Successfully ligated and transformed genes resulted in bands at 0.650 kb (heavy chains), 0.700 kb (kappa chains) and 0.590 kb (lambda chains) in gelelectrophoresis (Figure 12). For colonies with positive results in insert check PCRs, DNA was isolated from cultured E.coli and DNA was compared to sequencing results from PCR 2, whereby deviation led to picking of new colonies. For genes for which even after repeated picking of colonies no plasmid matching sequencing

results from PCR 2 could be isolated, cloning was not pursued. Overall, plasmid DNA was successfully isolated for 42 heavy chains, 21 kappa chains and 24 lambda chains, resulting in 45 potential recombinant monoclonal antibodies.

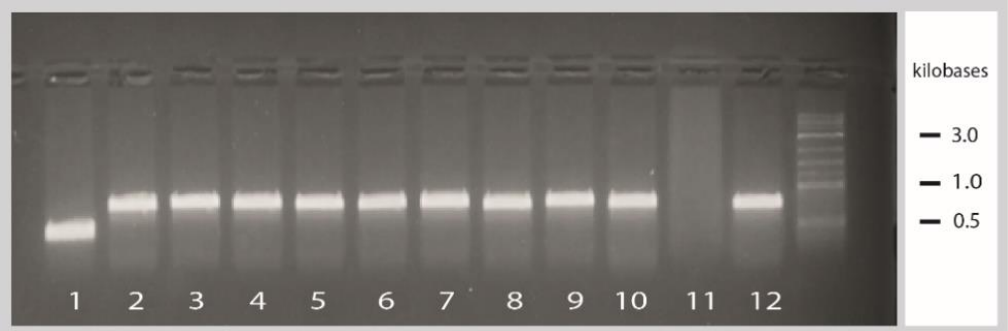

Figure 12: Products of insert check PCR. Exemplary samples are visualized using gel electrophoresis. Lanes 2-10 and 12 show bands at 0.650 kb representing amplified heavy chain vectors with likely ligated variable insert. Empty religated heavy vector with no insert results in band at 0.310 kb (Lane 1). Lane 11 shows no amplified DNA.

3.6 Transfection

Three days after transfecting HEK cells with our generated plasmids, we evaluated the success of transfection and presence of antibodies by analyzing harvested supernatants with ELISA. IgG concentrations were calculated from absorbance at 405 nm using the linear section of a four-parameter curve based on a serially diluted standard. For each sample, absorption was measured at two points in time (15 and 25 minutes after addition of substrate solution containing para-nitrophenyl phosphate) and in four different dilutions to then calculate the mean. Supernatants with concentrations below 1 µg/ml were regarded as negative. Positively tested supernatants were screened for reactivity. We were able to successfully express 41 out of 45 monoclonal antibodies, which were then screened for reactivity with concentrations ranging from 1.17 µg/ml to 18.15 µg/ml (Tables 31, 32).

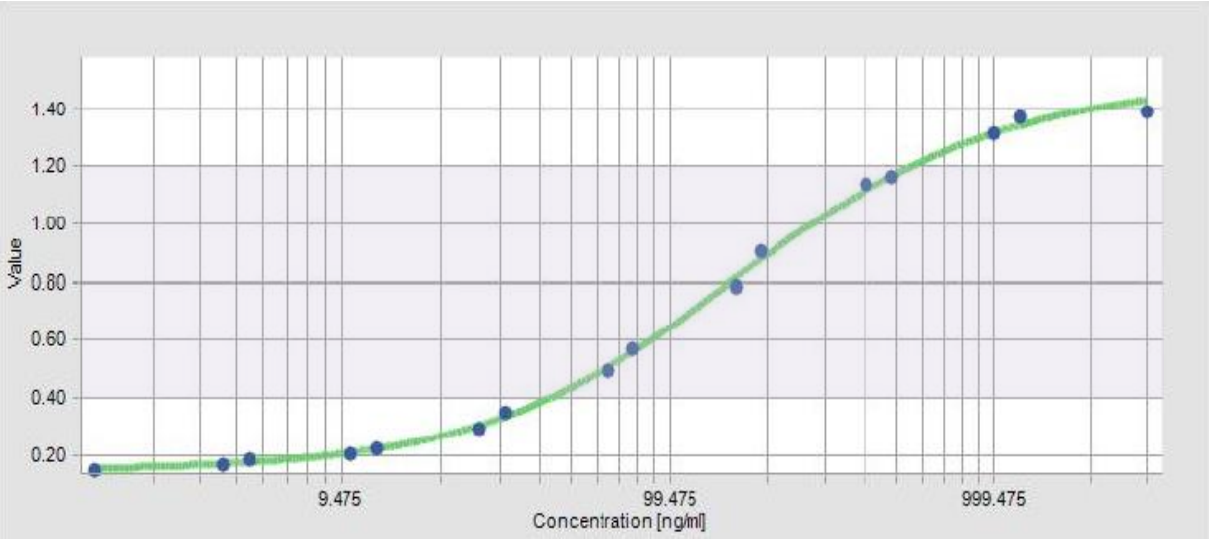

Figure 13: Antibody concentrations in supernatants measured with ELISA. Linear range (marked in purple) was determined as absorption at 405 nm between 0.40 and 1.20 for the exemplary samples displayed.

3.7 Screening for Reactivity

3.7.1 mGluR5

Among 27 expressed antibodies from patients with suspected anti-mGluR5 encephalitis, five (HL 136-143, HK 136-162, HK 136-169, HK 136-180, HK 136-187) showed characteristic mGluR5 patterns on murine brain sections. Antibody HL 136-143 provided a representative signal in the basal nuclei with emphasis on the striatum but without a signal in the corpus callosum (Figure 14, A). Antibody binding was strong in the hippocampus with emphasis on the Ammon's horn but with omission of the dental gyrus (Figure 14, D). No binding was observed in the cerebellum (Figure 14, G). This can be brought in line with mGluR5 expression as described in the literature (Shigemoto et al., 1993**;** Cai et al., 2019**).**

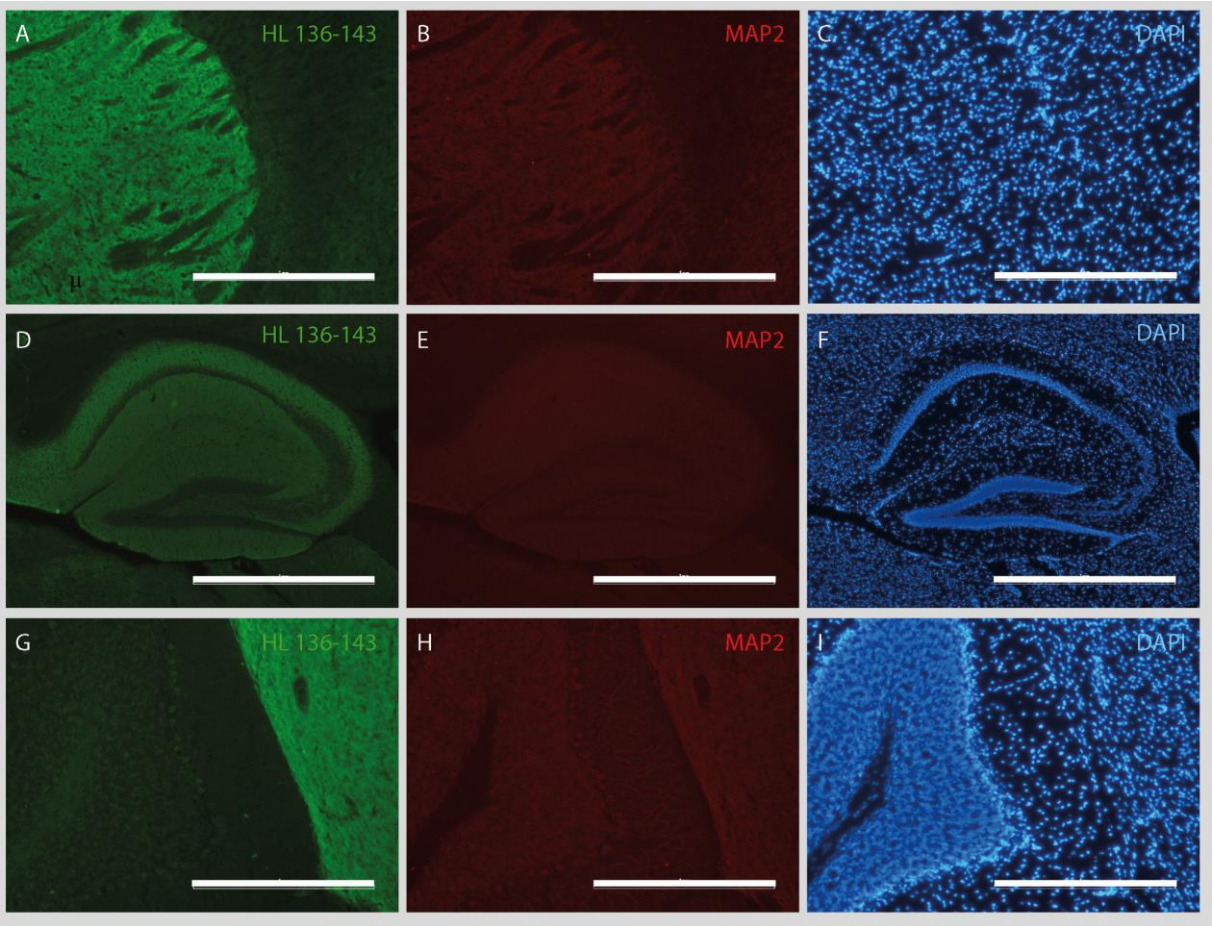

Figure 14: mGluR5 pattern on murine brain slices evoked by HL 136-143. This monoclonal antibody produces a strong signal in the striatum compared to a weak signal in the corpus callosum (A). A typical strong signal in the hippocampus with omission of the dental gyrus is presented in (D). Neither Purkinje cell layer, nor molecular layer nor granular layer are responsive to strong staining with HK 136-143 (G). Congruent image sections are displayed in each row for MAP2 as a neuronal marker (B, E, H) and DAPI to highlight nuclei (C, F, I). Scale bars: 267 µm in A, B, C, G, H, I; 1 mm in D, E, F.

For these five monoclonal antibodies, we furthermore proved binding to mGluR5 in a cell-based assay. Figure 15 illustrates the binding of antibody HL 136-143 in detail. The top row shows congruent images of mGluR5 transfected HEK cells. Transfection was confirmed by targeting the FLAG-Tag contained in the mGluR5 plasmid (B). HL 136-143 bound to these mGluR5 transfected HEK cells (C) in wide overlap with mGluR5 transfection (D). The bottom row shows untransfected HEK cells as a negative control with resulting absence of FLAG-Tag (F) and no binding of the applied monoclonal antibody (G). Figure 16 demonstrates analog binding behavior for the other four anti-mGLuR5 antibodies we generated: all of these antibodies bound to mGluR5 transfected HEK cells (C, G, K, O) in wide congruence with

mGluR5 transfection (D, H, L, P) but not to untransfected HEK cells (inlays C, G, K, O) as negative controls. In summary, we proved five of the monoclonal antibodies we generated to be reactive against mGluR5.

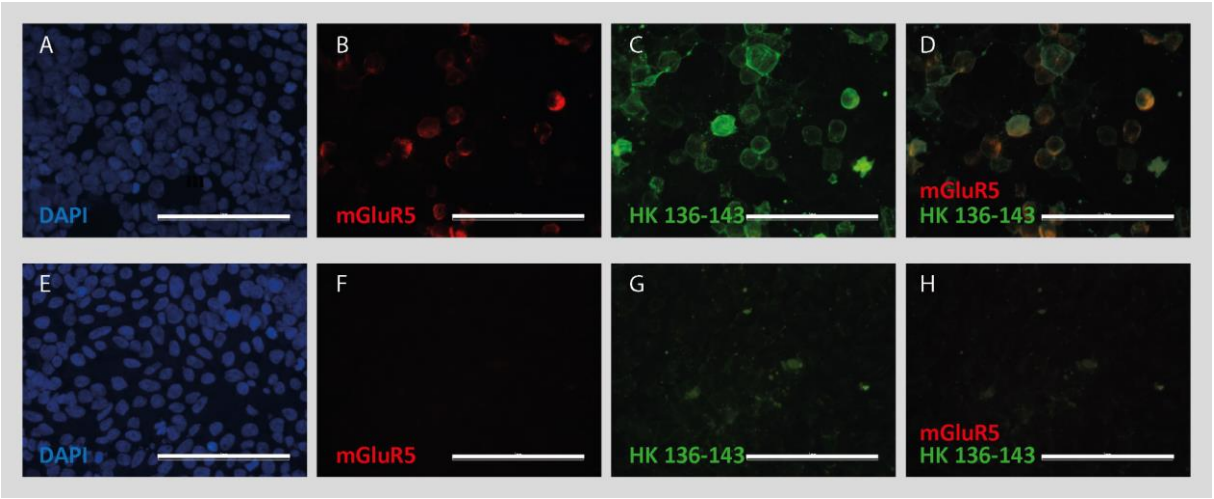

Figure 15: Testing monoclonal antibody HL 136-143 for reactivity against mGluR5. HEK cells in the top row were transfected with mGluR5 (A-D), while controls were untransfected (E-H). Monoclonal antibodies in supernatant bound to mGluR5 (C) but not to untransfected HEK cells (G). Staining against FLAG-Tag was used as a transfection control for mGluR5 (positive in B, negative in F). DAPI-mount visualizes cell nuclei (A, E). Overlayed images display a broad congruence of staining patterns of monoclonal human antibody and commercial anti-FLAG-Tag antibody on mGluR5 transfected HEK cells (D). Scale bars: 80 µm.

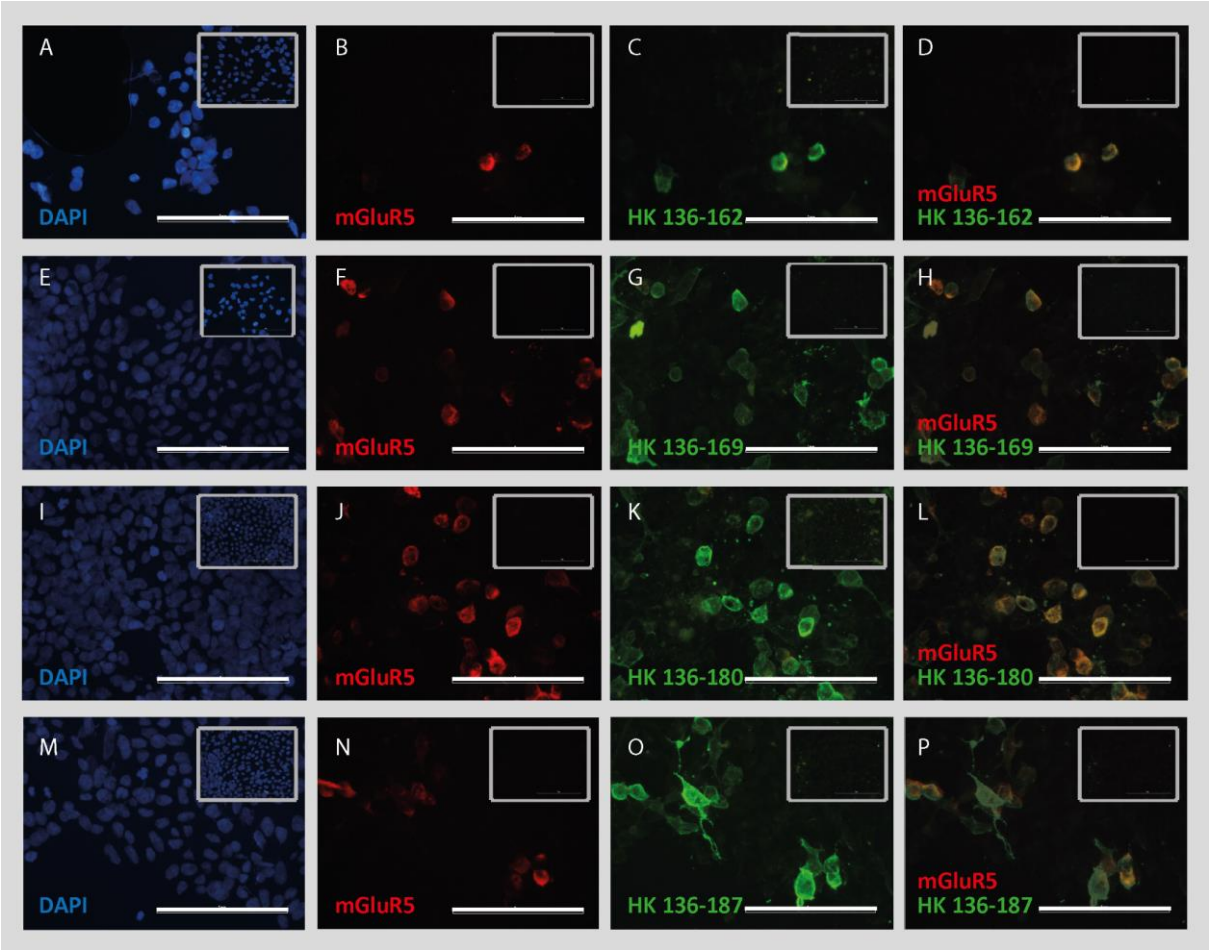

Figure 16: Testing monoclonal antibodies for reactivity against mGluR5. HEK cells were transfected with mGluR5 (A-P), while controls were untransfected (inserts in A-P). Antibodies HK 136-163 (A-D), HK 136-139 (E-H), HK 136-180 (I-L) and HK 136-187 (M-P) bound to mGluR5 but not to untransfected HEK cells. Merged images display a broad overlap of staining patterns of monoclonal human antibody and commercial anti-FLAG-Tag antibody on mGluR5 transfected HEK cells (D, H, L, P). Staining against FLAG-Tag was used as a transfection control (B, F, J, N). Scale bars 80 µm.

All of these mGluR5 reactive antibodies originated from patient AI-ENC 136. Bringing the mGluR5 reactive clones (HL 136-143, HK 136-162, HK 136-169, HK 136-180, HK 136-187) into line with the sequence analysis confirmed the special position of HL 136-143. It showed affinity to the target of interest, had a partner in clonal expansion (HL 136-181) and was one out of only two ASCs that originated from mGluR5 patients. However, the function of this related clone remains unknown as its antibody could not be expressed. Furthermore, the clonal relation between HK 136-169 and HK 136-187 proved relevant with both antibodies binding to mGluR5. The two remaining mGluR5 reactive clones HK 136-162 and HK 136-180 had not provided prominent characteristics in preceding sequencing. Except for ASC 136-143, all four

mGluR5 reactive cells were nMBC. All mGluR5 reactive antibodies were part of the dominating IgG1 subclass.

Besides the five antibodies identified to bind to mGluR5, another antibody from patient AI-ENC 136 was autoreactive within the CNS. When HEK cell supernatant containing antibody HK 136-149 was applied to murine brain slices, the coroid plexus was emphasized (Figure 17, D). Three antibodies originating from AI-ENC 82 showed autoreactivity against structures within the CNS when supernatants were screened (Figure 17). When supernatant of transfected HEK cells on murine brain sections was screened, one antibody (HK 082-113) generated a signal in the white matter emphasizing cerebellar white matter (Figure 17, A), internal capsule (B) and corpus callosum (C). Two further antibodies from patient AI-ENC 82 evoked a signal in the murine cerebellum: HK 82-129 bound to Purkinje cells (Figure 17, E) while HK 82-130 accentuated the molecular layer (Figure 17, F).

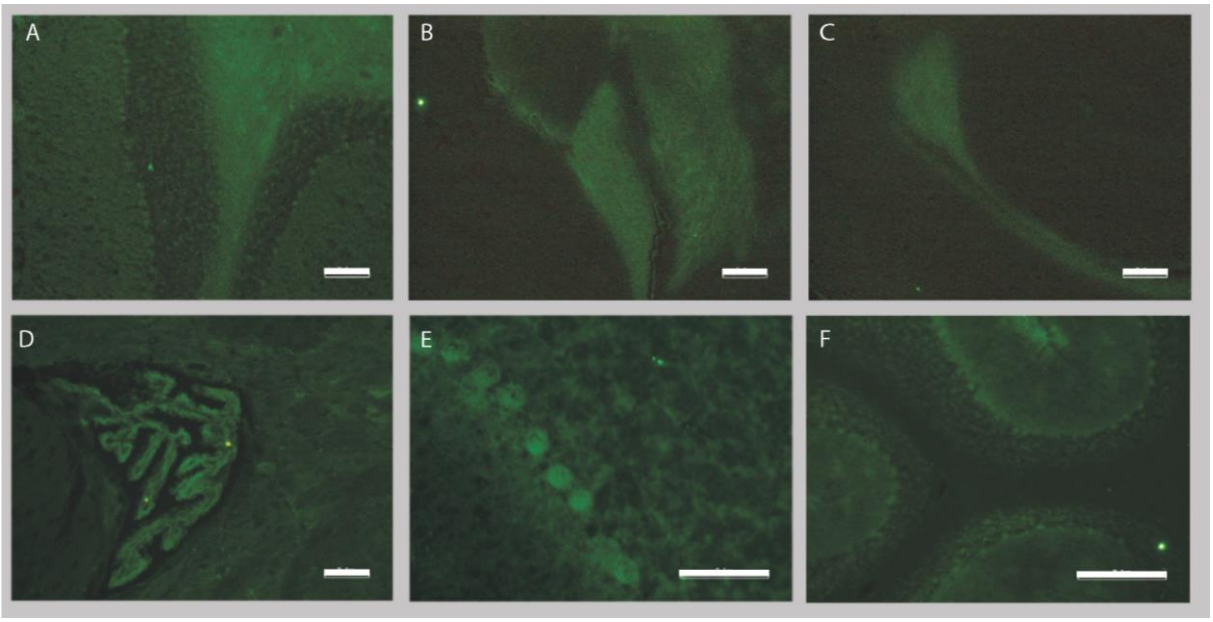

Figure 17: Reactivities of monoclonal antibodies from mGluR5 patients. HK 82-113 (A-C) shows white matter signal in cerebellum (A), internal capsule (B) and corpus callosum (C). HK 136-149 highlights the coroid plexus (D). HK 82-129 binds to Purkinje cells (E), while HK 82-130 stains the cerebellar molecular layer (F). Scale bars: 100 µm in A, B, D; 200 µm in C, F; 50 µm in E.

Table 31: Summarized reactivities of mGluR5 patients. All antibodies originate from patients with mGluR5-associated encephalitis. Reactivity: – negative, + weak positive, ++ strong positive.

Monoclonal antibody	Concentration of IgG in µg/ml used for testing	Tissue reactivity on murine brain sections	HEK cell-based assay	
			mGluR5	wild-type
HL 001-103	8.59	-	-	-
HL 001-106	-	-	-	-
HK 001-106	9.39	-	-	-
HL 001-116	1.71	-	-	-
HL 001-117	11.82	-	-	-
HL 001-118	12.53	-	-	-
HL 001-126	16.70	-	-	-
HK 82-103	16.70	-	-	-
HK 82-105	10.00	-	-	-
HK 82-113	18.15	++	-	-
HK 82-129	11.82	+	-	-
HK 82-130	17.05	+	-	-
HL 148-104	10.00	-	-	-
HL 148-111	18.15	-	-	-
HL 148-112	9.47	-	-	-
HL 136-103	4.37	-	-	-
HK 136-133	4.42	-	-	-
HL 136-143	13.7	++	++	-
HK 136-149	1.51	+	-	-
HL 136-161	5.28	-	-	-
HK 136-162	3.12	++	++	-
HK 136-169	6.26	++	++	-
HL 136-171	1.17	-	-	-
HK 136-180	6.86	++	++	-
HL 136-180	4.49	-	-	-
HK 136-184	2.05	-	-	-
HK 136-186	3.67	-	-	-
HK 136-187	7.82	++	++	-
HL 136-196	-	-	-	-

3.7.2 Progranulin

The 14 potential anti-Progranulin antibodies were also tested using a cell-based assay (Figure 19). Transfection of HEK cells was confirmed by using a plasmid encoding both for Progranulin and GFP (A, D, G, J). A commercial anti-Progranulin antibody serving as a positive control bound to these HEK cells (B) in broad overlap with transfection (C). Using only secondary antibody as a negative control resulted in no binding (K, L). Thirteen of our potential anti-Progranulin antibodies did not bind to HEK cells at all as exemplified for antibody HK 158-178 (D, E, F). Antibody HL 158-213 bound to these HEK cells (H) but not in overlap with Progranulin transfection (I). All 14 antibodies were additionally tested against Progranulin in an ELISA-based approach externally at AG Lorenz Thurner, José-Careras Zentrum, Homburg, where none of the antibodies showed binding to Progranulin. Overall, none of the created monoclonal antibodies were directed against Progranulin.

We did identify three clones among the antibodies retrieved from patients with Progranulin-associated encephalitis to be reactive against structures within the CNS. Screening of HEK cell supernatant containing the following antibodies revealed positive results on murine brain sections. Antibody HK 158-107 evoked a signal in the cerebellum by targeting Purkinje cells (Figure 18, A). Small blood vessels within the murine brain were emphasized by antibody HK 158-178 (Figure 18, B). HL 158-241 was found to bind to the cerebellar molecular layer (Figure 18, C).

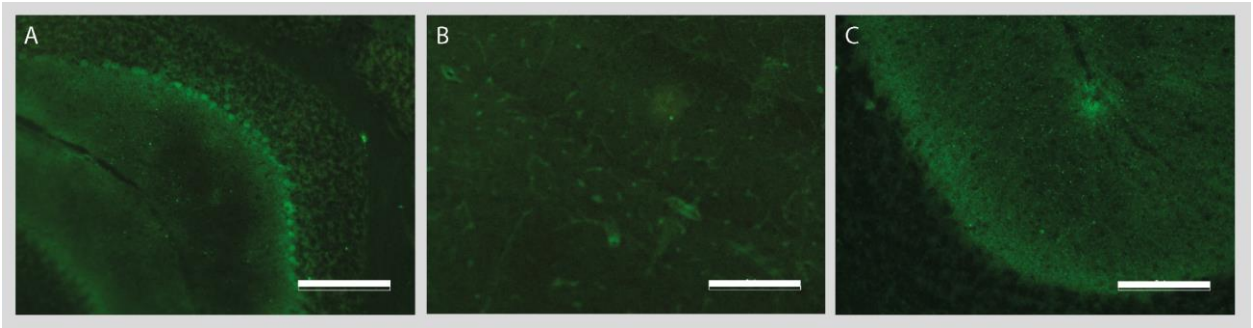

Figure 18: Reactivities of monoclonal antibodies from Progranulin patients. HK 158-107 accentuates Purkinje cells (A). HK 158-178 binds to small vessels (B). C shows cerebellar staining of HL 158-241 with its affinity to the molecular layer. Scale bars: 200 µm in A, 100 µm in B and C.

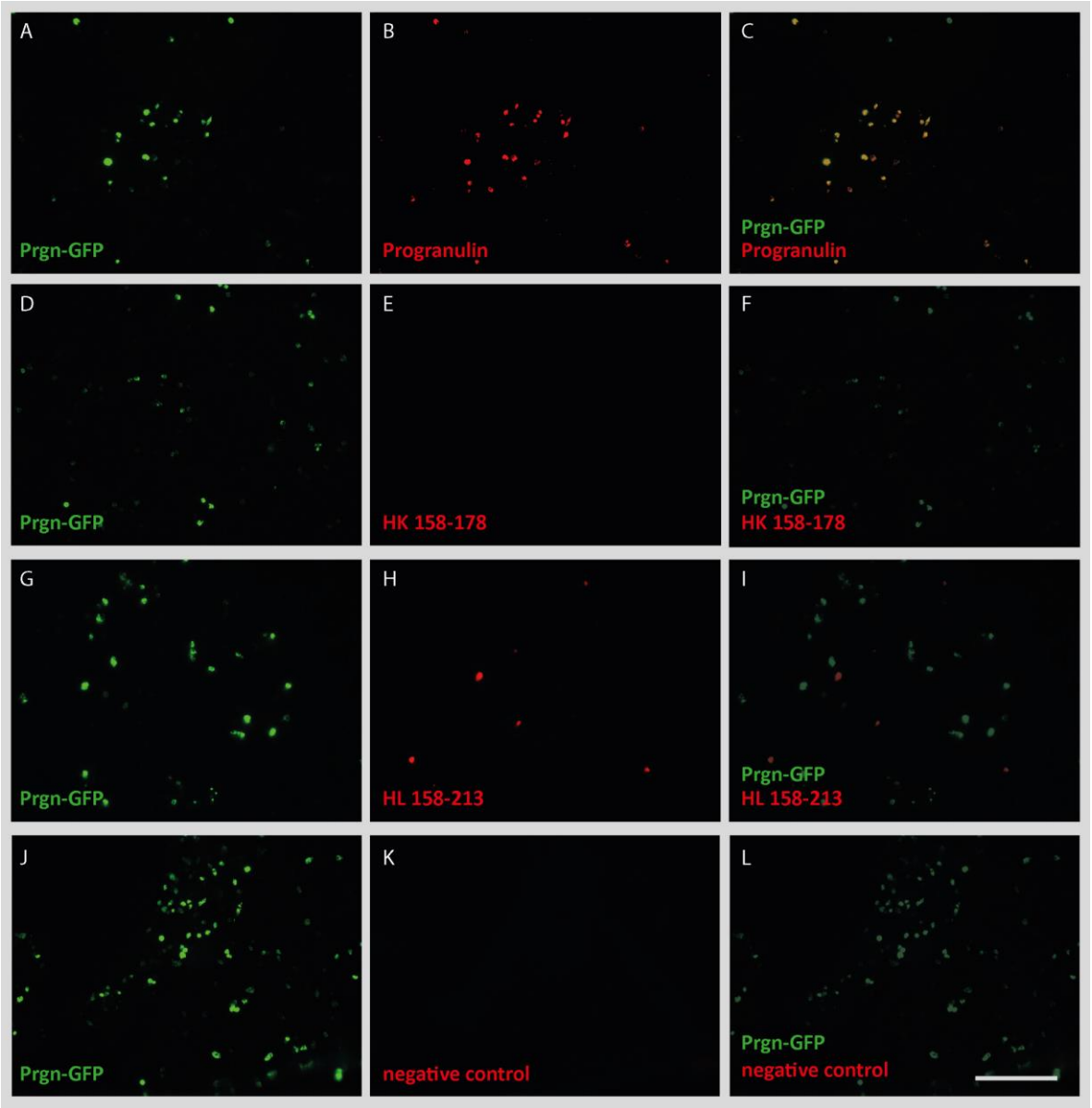

Figure 19: Testing monoclonal antibodies for reactivity against Progranulin. All HEK cells shown were transfected with Progranulin-GFP, which allowed transfection control (A, D, G, J). A commercial anti-Progranulin antibody bound to transfected HEK cells (B) in wide congruence with Progranulin transfection (C). Monoclonal antibody HL 158-178 did not bind to Progranulin transfected HEK cells (E, F). Monoclonal antibody HL 158-213 did bind to HEK cells, but not in congruence with Progranulin transfection (H, I). The bottom row serves as a negative control showing that secondary antibody alone does not bind to any cells (K, L). Scale bar: 200 µm.

Table 32: Summarized reactivities of Progranulin patients. All antibodies originate from patients with Progranulin-associated encephalitis. Reactivity: – negative, + weak positive, ++ strong positive.

Monoclonal antibody	Concentration of IgG in µg/ml used for testing	Tissue reactivity on murine brain sections	HEK cell-based assay	
			Progranulin	wild-type
HK 158-104	49.73	-	-	-
HK 158-107	26.16	+	-	-
HL 158-117	-	-	-	-
HL 158-156	8.55	-	-	-
HL 158-158	10.92	-	-	-
HK 158-178	16.64	++	-	-
HK 158-191	8.59	-	-	-
HK 158-211	8.49	-	-	-
HL 158-213	1.71	-	-	+
HK 158-216	12.53	-	-	-
HL 158-216	-	-	-	-
HL 158-237	1.45	-	-	-
HL 158-241	16.70	+	-	-
HL 158-251	10.0	-	-	-
HL 159-113	18.15	-	-	-
HK 159-147	1.48	-	-	-

3.8 Fab Fragments

Having generated monoclonal antibodies against mGluR5 from patients with autoimmune encephalitis, we next developed a specific remedy for these autoreactive antibodies. Referring to Hughes et al. (2010), we chose the strategy of creating Fab fragments with identical antigen-binding sites to the full IgG antibodies we had created to then displace harmful full IgG antibodies with their corresponding Fab fragments. To establish the concept of generating and applying such Fab fragments, we made use of antibody HL 003-102 which is a monoclonal antibody against the NMDAR generated in our lab and a well-characterized model antibody in our group (Kreye et al., 2016; Ly et al., 2018; Jurek et al., 2019). We successfully generated a Fab fragment of antibody HL 003-102: using the plasmid encoding for the full IgG heavy chain of HL 003-102 as a template, we applied a PCR strategy, introducing a stop codon to shorten the constant region of the antibody and a FLAG-Tag with primers. The plasmid encoding for the corresponding light chain was left unchanged, as Fab fragments contain a full light chain. This PCR product encoding for a shortened Fab heavy chain with FLAG-Tag was cloned into the IgG1 expression vector for heavy chains described above (Chapter 2.6.2.2). Plasmid could be isolated from E.coli after transformation and

sequencing confirmed the desired sequence. Three days after transfection of HEK cells with this plasmid, while co-transfecting the regular corresponding light chain, HEK cells expressed the Fab fragment as shown by staining against FLAG-Tag (Figure 20).

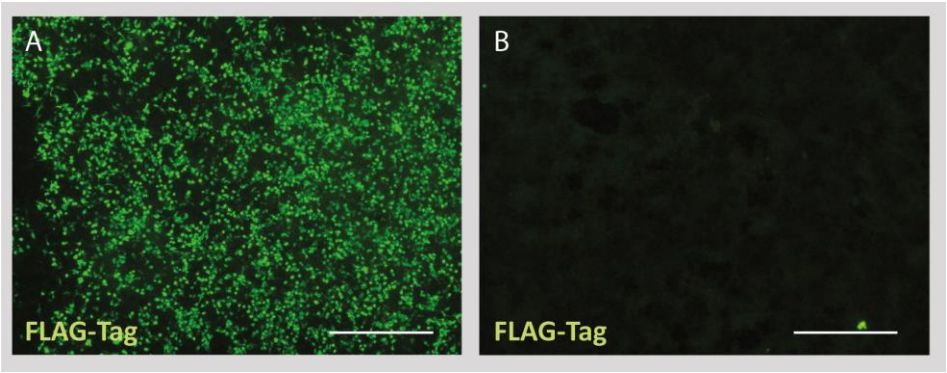

Figure 20: Expression of Fab fragments in HEK cells. Transfected HEK cells expressed Fab fragments, visualized by targeting contained FLAG-Tag (A). Untransfected HEK cells stained for FLAG-Tag showed no signal (B). Scale bars: 500 µm.

Supernatant harvested from such transfected HEK cells evoked a staining pattern on murine brain slices identical to the pattern caused by the corresponding full IgG antibodies. We visualized binding by application of fluorophore-conjugated secondary antibody targeting the FLAG-Tag contained in the Fab fragments (Figure 21).

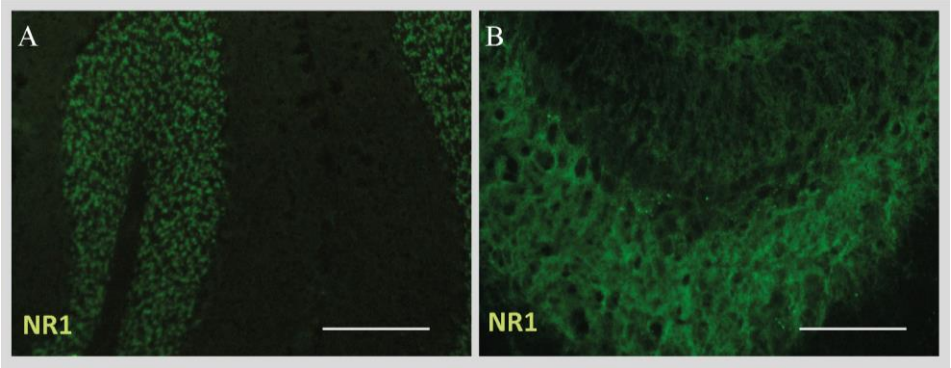

Figure 21: Immunohistochemistry of Fab 003-102. Characteristic NR1 pattern defined by binding to granule cells (A) and hippocampal neuropil with omission of dentate gyrus (B). Scale bars: 200 µm in A, 100 µm in B.

With confirmed reactivity of the Fab fragments, we tested whether these Fab fragments could compete with full IgG for shared binding sites. To do so, full IgG of antibody HL 003-102 was conjugated with CruzFluor488 succimidyl ester with a ratio of 8.5 molecules dye per molecule IgG. This conjugated antibody showed a characteristic NR1 pattern on unfixed murine brain slices (Figure 22). In a next step, Fab fragments eluted from anti-FLAG beads were capable of displacing full IgG of the same antibody on murine brain slices in a concentration-dependent manner, demonstrated by a decreasing signal of fluorophore-conjugated full IgG (Figure 23). We here demonstrated that full IgG of this NR1-antibody and corresponding Fab fragments with identical antigen-binding site do compete for epitopes, resulting in less binding of harmful full IgG antibodies on murine brain sections.

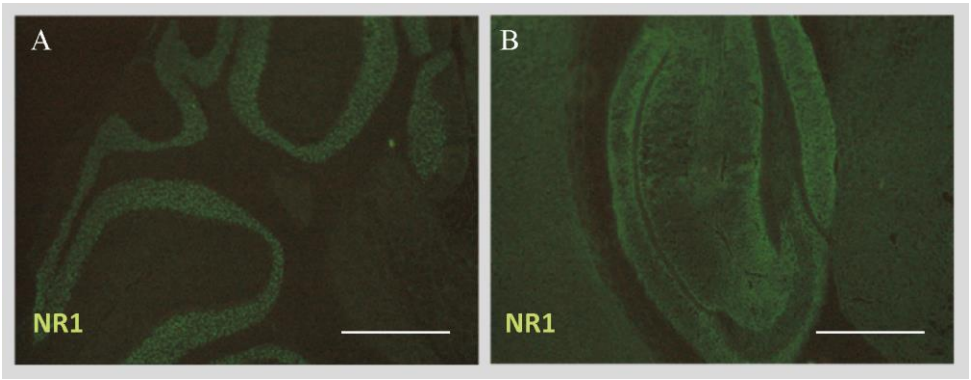

Figure 22: Immunohistochemistry of full IgG HL 003-102. Typical NR 1 signal in visible in granule cells (A) as well as in the hippocampal neuropil (B). Scale bars: 500 µm.

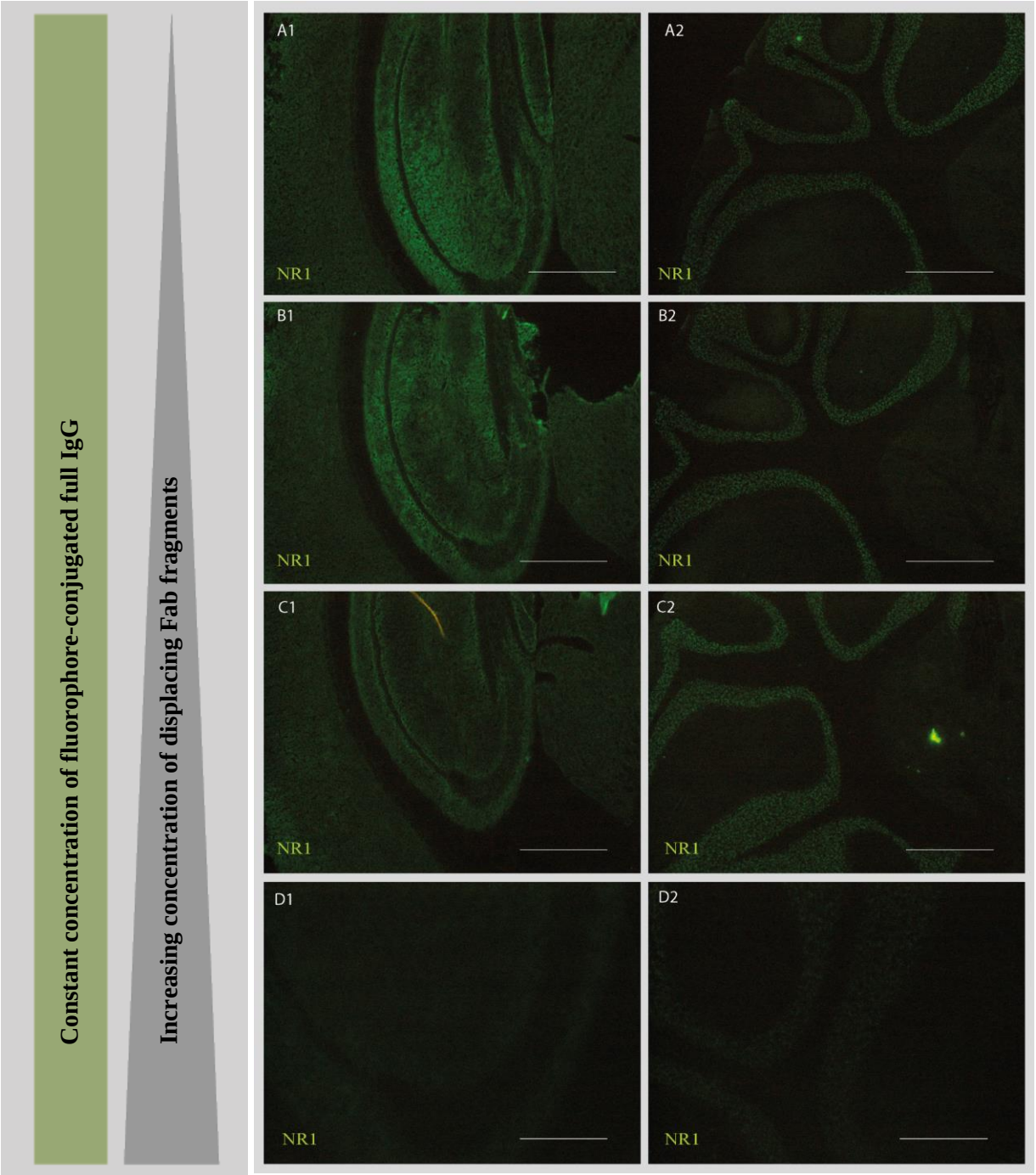

Figure 23: Displacement of full IgG by Fab fragments. Concentrations of full IgG HL 003-102 (fluorophore-conjugated) remained constant at 0.09 µg/ml. Increasing concentrations of Fab 003-102 from A to D (A: 0.0059 µg/ml, B: 0.059 µg/ml, C: 0.59 µg/ml, D: 5.9 µg/ml) resulted in a decreasing signal of conjugated full IgG. Scale bars: 500 µm in A-C; 166,67 µm in D1; 250 µm in D2.

4 Discussion

4.1 Evaluation of Hypothesis I

We hypothesized that we could generate monoclonal antibodies against mGluR5 and Progranulin from patient CSF and we partly succeeded. We generated five monoclonal cell lines producing antibodies against mGluR5 and in doing so proved autoimmune reactivity against mGLuR5 on a monoclonal level. All antibodies with this reactivity stemmed from one CSF sample of one patient (AI-ENC 136). We could therefore describe a multi-clonal immune response directed against mGluR5 for this patient. The genetic information retrieved from these clones can be aligned with prior research regarding immunoglobulin class distribution: all five antibodies are of isotype IgG1, which is the main type of immunoglobulins in mGluR5 encephalitis (Spatola et al., 2018). Identification of cell type and immunoglobulin class allows some conclusions about the role of a cell. ASCs result from antigen stimulation (Cruse & Lewis, 2004). One of the mGluR5-reactive antibodies (HL 136-143) originating from an ASC therefore strengthens the hypothesis that autoimmune reactivity against mGluR5 played a central role in pathogenesis in this patient. The monoclonal antibodies we created are not only proof of the diagnosis, they above all allow progress in understanding disease mechanisms. We can now provide five monoclonal antibodies against mGluR5 in large amounts for functional testing. Spatola et al. (2018) showed that decrease of mGluR5 occurs when cultured neurons are exposed to IgG of patients with mGluR5 encephalitis. Consolidating and specifying such experiments with the now available purified monoclonal antibodies against mGluR5 must be the next steps to understand this downregulation, identify further disease mechanisms and define the role of single clones. With unlimited amounts of monoclonal antibodies, modulating factors such as exposure time or IgG concentration can be investigated. Purified IgG can be used to establish in vivo models of anti-mGluR5 encephalitis, for instance by intrathecal application in rodents. Not only can brains of sacrificed animals be analyzed for disease effects with histopathological methods, but clinical phenotypes can be investigated and diagnostics and therapy options can be evaluated in such a disease model.

However, we did not succeed in retrieving and cloning mGluR5 reactive cells based on the three CSF samples we had from other patients, even though samples from these patients had previously proven reactivity against this epitope. A range of errors is in line for failure at this point: if weak spots are analyzed chronologically, the first source of error may be the sample itself. A positive immunostaining of the supernatant of the very same sample requires only presence of antibodies

against mGluR5, but our protocol relies on cells as a starting product. In short, the samples, furthermore only representing a relatively small volume of a patient's CSF, may simply not have contained cells of interest. This is supported by the fact that the sample we did successfully clone cells from was the one with the highest cell count by far. Secondly, immune cells in CSF are sensitive to changes in environment regarding temperature, osmolarity and metabolic state and may have been impaired during sample storage or preparation. Furthermore, the sample had to undergo numerous steps of pipetting, centrifuging and washing during the staining for surface markers to prepare for sorting with each step, which was a risk for losing cells. Another source of cell loss was the single cell sorting itself due to technical reasons. PCR efficiencies were comparably low and possible candidates may have been sorted out, but we did not succeed in amplifying their DNA. This effect is intensified as repeated inability to amplify one chain makes it necessary to disregard the whole cell, even though one chain type may have been successfully amplified.

All the weak spots described above also apply to our unsuccessful attempt at generating monoclonal antibodies against Progranulin. In this case, we did not succeed in generating any antibodies, and we must consider a more systematic failure. When sorting cells originating from these samples, there was a high background of PE-conjugated anti-CD138 antibodies which may have led to selection of cells with expression of CD138 lower than measures. The resulting workup of such irrelevant cells that were mistaken for ASCs can be an explanation for our inability to generate monoclonal antibodies based on these cells.

4.2 Limitations in Analyzing Monoclonal Antibody Repertoires

The entire procedure of analyzing the antibody repertoire of a patient is based on one CSF sample of varying size and with a limited number of contained cells. Absence of a cell in our workup does not exclude the possibility of its presence in the CSF of a patient in vivo. Throughout the process of generating monoclonal antibodies from a CSF sample to recombinant immunoglobulins, numerous candidates were eliminated for different reasons such as reoccurring artificial mutations when amplifying the genes, unsuccessful amplification or the inability to express an antibody in HEK cells. With only a limited share of sorted cells resulting in a monoclonal cell line, the ability to draw inferences about the frequency of occurrence of a cell in vivo is limited.

We have proven reactivity against mGluR5 using a cell-based assay for five of the antibodies we generated. It is within the realms of possibility that a proven reactivity of a cell and its antibodies, respectively, is a mere co-reactivity of a cell that in fact results from stimulation with a different antigen (Van Regenmortel, 2014). However, this seems highly improbable as we identified five different cells from this patient with reactivity against mGluR5.

For eight cells, amplification was successful for both kappa and lambda chains, although cells in vivo usually express only either a lambda or kappa chain (Cruse & Lewis, 2004). However, the presence of cells featuring both kappa and lambda chains has been demonstrated in human peripheral blood (Giachino et al., 1995). With the protocol we carried out, it was impossible to reconstruct whether both chain types were expressed in vivo or whether the amplification was based on contamination.

4.3 Further Autoantigens Within and Outside of the CNS

Screening of generated monoclonal antibodies revealed various autoreactivities within the CNS that did not match the expected reactivities against mGluR5 and Progranulin, respectively. This can be aligned with prior findings regarding autoimmune encephalitis, where numerous autoantigens in one patient could be identified (Kreye et al., 2016).

Antibody HK 082-113 originated from a patient with autoreactivity against mGluR5 but does not bind to mGluR5 itself. Certainly, it does bind to murine brain sections in immunohistochemistry staining white matter (Figure 17). Based on the pattern displayed on murine brain sections, the antibody could possibly interact with myelination. Interaction of the immune system with myelin is often discussed in conjunction with the pathogenesis of multiple sclerosis (Lubetzki & Stankoff, 2014). Nevertheless, such autoantibodies targeting myelin antigens do not necessarily have to be noxious but can even enhance remyelination (Warrington et al., 2007). This antibody is therefore worth investigating further not only for a deeper understanding of the disease mechanisms in this patient, but also to examine potential effects it may have on myelination and demyelination. To identify the unknown epitope bound by such CNS autoreactive antibodies, mass spectrometry can be a method to identify antibody targets (P. Wang & Wilson, 2013). Another interesting candidate for deeper investigation, besides the CNS reactive antibodies, is HL 158-213 due to its binding behavior in cell-based assays (Figure 19). Intending to test it against Progranulin, we found it to

bind to comparably small and condensed HEK cells under omission of those cells for which transfection of Progranulin had been successful. We thus assume that expression of the epitope it binds to might be enhanced in apoptotic cells. Cells undergoing programmed cell death are a common target for the immune system as their elimination is essential to securing function in organ systems (Grönwall et al., 2014). Interestingly, the antibody we describe has 22 SHM and is therefore far from germline configuration as pre-described for naturally occurring antibodies interacting with apoptosis-associated epitopes (Grönwall et al., 2014).

4.4 Evaluation of Hypothesis II

We successfully generated Fab fragments with variable regions identical to those contained in full IgG of an antibody with reactivity to the NR1 subunit of the NMDAR. We demonstrated binding of these Fab fragments to NR1 both on transfected HEK cells and murine brain sections evoking a staining pattern identical to the one caused by the corresponding full IgG antibodies. Hughes et al. (2010) had shown that Fab fragments bind to the NMDAR. We proved that they compete with full IgG: when adding Fab fragments in high concentrations at the same time, full IgG bound to the target on murine brain tissue to a lesser degree. Decrease of surface NMDAR is an Fc-dependent mechanism in anti-NMDAR encephalitis (Hughes et al., 2010). If these two trains of thought are joined together, this toxic downregulation could potentially be attenuated by displacing full IgG with Fab fragments. To investigate this, experiments will have to be pursued using neuronal cell cultures featuring serial dilutions of Fab fragments and full IgG, with the hypothesis that Fab fragments could possibly diminish the decrease of surface NMDAR caused by full IgG antibodies in a concentration-dependent manner.

We used an antibody well characterized and established in our group as a template to create Fab fragments with identical antigen-binding sites. This antibody has a high affinity to NR1 (Ly et al., 2018). It was legitimate to use this antibody to build on the preexisting research on Fab fragments performed in anti-NMDAR encephalitis by Hughes et al., (2010). As the archetypical type of autoimmune encephalitis, we established the concept of Fab fragments in anti-NMDAR encephalitis first. However, the methods we describe can now be applied to generate Fab fragments of any of the monoclonal full IgG antibodies generated with our protocol. Using the plasmids encoding for the anti-mGluR5 antibodies generated in the context of this dissertation as a template, for instance, Fab fragments directed against mGluR5 can be produced. Creating not only a full

IgG repertoire of a patient's CSF sample but also a Fab fragment repertoire will allow investigation of pathomechanisms caused by individual antibodies and a distinction between Fc-dependent and Fc-independent antibody effects in subsequent experiments. Little is known about the molecular mechanisms induced by anti-mGluR5 antibodies. However, receptor downregulation upon antibody binding to mGluR5 has been described (Spatola et al., 2018). It has yet to be investigated whether this decrease in surface mGluR5 is based on crosslinking the Fc parts of antibodies as shown for the decrease of surface NMDAR by Hughes et al. (2010) and therefore might be susceptible to intervention with Fab fragments.

4.5 Monoclonal Fab Fragments as a Useful Scientific Tool

We have shown here that Fab fragments can displace harmful full IgG antibodies, but much more has to be taken into account when striving to model such a displacement in an in vivo scenario. In our in vitro setting, Fab fragments and full IgG were applied at the same time in the sense of competition for binding sites, whereas in an in vivo scenario, full IgG would be present before adding Fab fragments. As we did not conduct an experiment with this chronology, we cannot confirm that Fab fragments could actively displace their corresponding full IgG molecules when they have bound beforehand. But such an effect does not seem far-fetched as antibody-antigen interaction relies on non-covalent attachment and is amenable to influence (Janeway CA Jr et al., 2001). Furthermore, NMDAR as the archetypical target in autoimmune encephalitis is constantly recycled in the sense of synaptic plasticity (Lau & Zukin, 2007). Binding of harmful antibodies must therefore be a continuous process throughout the course of disease, which makes it susceptible to interference with Fab fragments.

Common treatment for autoimmune encephalitis available at this point is based on affecting the immune system as a whole in the form of plasma exchange, intravenous immunoglobulin or corticosteroids as first-line and Rituximab or Cyclophosphamide as second-line therapy (Dalmau & Rosenfeld, 2014). Newer strategies include the proteasome inhibitor Bortezomib, modulation of the immune response by targeting the IL-6 receptor, and application of IL-2 (Shin et al., 2018). Still, none of these therapeutic strategies have the ability to target exclusively harmful antibodies. Fab fragments with variable regions specifically matching epitopes in autoimmune encephalitis might be able to remedy antibody effects more specifically by blocking binding sites for toxic full IgG. However, such an effect is a theoretical construct at this point and still has to be investigated.

Moreover, the therapeutical potential of such displacement would be limited to Fc-dependent disease mechanisms.

The displacing effects proven here are based on identical antigen-binding domains of full IgG and Fab fragments. Patients have both intraindividually and interindividually diverse antibodies. One autoantigen may feature numerous binding sites and a variety of immunoglobulins may occur even to one epitope within the frame of a polyclonal immune response. This underlines the utility of patient-derived monoclonal Fab fragments for further investigation of disease mechanisms as this allows discrimination of individual antibody effects. For a hypothetical therapeutic application, however, it would constitute another obstacle: to oppose all of these antibodies, an individual analysis and even individual cloning would have to be performed for each patient, which goes far beyond the constraints of routinely applied treatment. An easier albeit less specific and less yielding approach could be the digest of a patient's antibodies with papain to create Fab fragments as conducted by Hughes et al. (2010).

4.6 Concluding Remarks

Overall, we have not only proved autoreactivity against mGluR5 in a patient with autoimmune encephalitis on a monoclonal level, but have also supplied information regarding these reactive clones including cell type, immunoglobulin class, gene family usage and SHM. We furthermore have provided monoclonal cell lines producing recombinant antibodies to reconstruct the polyclonal immune response in anti-mGluR5 encephalitis. These monoclonal antibodies can be generated in large amounts and thus can be made available for thorough investigation of pathomechanisms in vitro and in vivo. Moreover, we have paved the way for further investigation of individual antibody effects and a potential strategy to remedy antibody effects in autoimmune encephalitis by demonstrating that Fab fragments can displace noxious full IgG antibodies with identical antigen-binding sites. We proved this displacement for antibodies against the NMDAR as the archetype of autoantigens in this group of diseases. However, we here provide a new strategy for generating monoclonal Fab fragments that can be applied to create Fab fragments based on plasmids encoding for numerous immunoglobulins and therefore be of use in various contexts.

References

Benussi, L., Ghidoni, R., Pegoiani, E., Moretti, D. V., Zanetti, O., & Binetti, G. (2009). Progranulin Leu271LeufsX10 is one of the most common FTLD and CBS associated mutations worldwide. *Neurobiology of Disease*, *33*(3), 379–385.

Bhandari, V., Palfree, R. G., & Bateman, A. (1992). Isolation and sequence of the granulin precursor cDNA from human bone marrow reveals tandem cysteine-rich granulin domains. *Proceedings of the National Academy of Sciences of the United States of America*, *89*(5), 1715–1719.

Blinder, T., & Lewerenz, J. (2019). Cerebrospinal fluid findings in patients with autoimmune encephalitis-a systematic analysis. *Frontiers in Neurology*, *10*, 804.

Cai, G., Wang, M., Wang, S., Liu, Y., Zhao, Y., Zhu, Y., Zhao, S., Zhang, M., Guo, B., Yao, H., Wang, W., Wang, J., & Wu, S. (2019). Brain mGluR5 in Shank3B−/− Mice Studied With in vivo [18F]FPEB PET Imaging and ex vivo Immunoblotting. *Frontiers in Psychiatry*, *10*, 38.

Carr, I. (1982). The Ophelia Syndrome: Memory Loss in Hodgkin's Disease. *The Lancet*, *319*(8276), 844–845.

Cenik, B., Sephton, C. F., Kutluk Cenik, B., Herz, J., & Yu, G. (2012). Progranulin: a proteolytically processed protein at the crossroads of inflammation and neurodegeneration. *The Journal of Biological Chemistry*, *287*(39), 32298–32306.

Cruse, J. M., & Lewis, R. E. (2004). *Atlas of Immunology*. https://books.google.de/books?id=L4CI-qkhuQ8C&pg=PA157&dq=b+cell+maturation&hl=sv&sa=X&ved=0ahUKEwjkprb4tJblAhXN_aQKHWcMBcIQ6AEIMDAB#v=onepage&q=B cell maturation&f=false, last date accessed: 2020-05-13, 09.20am

Dalmau, J., & Rosenfeld, M. R. (2014). Autoimmune encephalitis update. *Neuro-Oncology*, *16*(6), 771–778.

Daneman, R., & Prat, A. (2015). The blood-brain barrier. *Cold Spring Harbor Perspectives in Biology*, *7*(1), a020412.

Daniel, R., He, Z., Carmichael, K. P., Halper, J., & Bateman, A. (2000). Cellular Localization of Gene Expression for Progranulin. *Journal of Histochemistry & Cytochemistry*, *48*(7), 999–1009.

Darnell, R. B., & Posner, J. B. (2011). Paraneoplastic Syndromes. *Oxford University Press*. https://books.google.de/books?hl=de&lr=&id=H5XLSPrCtB4C&oi=fnd&pg=PP1&dq=Darnell+RB,+Posner+JB.+Paraneoplastic+Syndromes.+New+York:+Oxford%3B+2011&ots=QO79Zi-ZTW&sig=5xm-bIt5mGZsSfHQaSvp0qXOZJQ#v=onepage&q=Darnell RB%2C Posner JB. Paraneoplastic Syndromes, last date accessed: 2020-05-13, 09.23am

Dubey, D., Pittock, S. J., Kelly, C. R., McKeon, A., Lopez-Chiriboga, A. S., Lennon, V. A., Gadoth, A., Smith, C. Y., Bryant, S. C., Klein, C. J., Aksamit, A. J., Toledano, M., Boeve, B. F., Tillema, J. M., & Flanagan, E. P. (2018). Autoimmune encephalitis epidemiology and a comparison to infectious encephalitis. *Annals of Neurology*, *83*(1).

Esposito, S., Principi, N., Calabresi, P., & Rigante, D. (2019). An evolving redefinition of autoimmune encephalitis. *Autoimmunity Reviews*, *18*(2), 155–163.

Esterlis, I., Holmes, S. E., Sharma, P., Krystal, J. H., & DeLorenzo, C. (2018). mGluR5 and Stress Disorders: Knowledge Gained from Receptor Imaging Studies. *Biological Psychiatry*, *84*(2), 95.

Ghidoni, R., Benussi, L., Glionna, M., Franzoni, M., & Binetti, G. (2008). Low plasma progranulin levels predict progranulin mutations in frontotemporal lobar degeneration. *Neurology*, *71*(16), 1235–1239.

Giachino, C., Padovan, E., & Lanzavecchia, A. (1995). κ+γ+ Dual receptor B cells are present in the human peripheral repertoire. *Journal of Experimental Medicine*, *181*(3), 1245–1250.

Giudicelli, V., Chaume, D., & Lefranc, M.-P. (2005). IMGT/GENE-DB: a comprehensive database for human and mouse immunoglobulin and T cell receptor genes. *Nucleic Acids Research*, *33*(Database issue), D256-61.

Gregory, K. J., Noetzel, M. J., & Niswender, C. M. (2013). Pharmacology of metabotropic glutamate receptor allosteric modulators: Structural basis and therapeutic potential for CNS disorders. In *Progress in Molecular Biology and Translational Science* (Vol. 115, pp. 61–121). Elsevier B.V.

Grönwall, C., Charles, E. D., Dustin, L. B., Rader, C., & Silverman, G. J. (2014). Selection of apoptotic cell specific human antibodies from adult bone marrow. *PloS One*, *9*(4), e95999.

Guan, H.-Z., Ren, H.-T., & Cui, L.-Y. (2016). Autoimmune Encephalitis: An Expanding Frontier of Neuroimmunology. *Chinese Medical Journal*, *129*(9), 1122–1127.

He, Z., & Bateman, A. (2003). Progranulin (granulin-epithelin precursor, PC-cell-derived growth factor, acrogranin) mediates tissue repair and tumorigenesis. *Journal of Molecular Medicine*, *81*(10), 600–612.

Hughes, E. G., Peng, X., Gleichman, A. J., Lai, M., Zhou, L., Tsou, R., Parsons, T. D., Lynch, D. R., Dalmau, J., & Balice-Gordon, R. J. (2010). Cellular and synaptic mechanisms of anti-NMDA receptor encephalitis. *The Journal of Neuroscience : The Official Journal of the Society for Neuroscience*, *30*(17), 5866–5875.

Janeway CA Jr, Travers P, Walport M, et al. (2001). *The interaction of the antibody molecule with specific antigen - Immunobiology - NCBI Bookshelf*. Garland Science. https://www.ncbi.nlm.nih.gov/books/NBK27160/, last date accessed: 2020-08-13, 09.26am

Jessen, N. A., Munk, A. S. F., Lundgaard, I., & Nedergaard, M. (2015). The Glymphatic System: A Beginner's Guide. *Neurochemical Research*, *40*(12), 2583–2599.

Jurek, B., Chayka, M., Kreye, J., Lang, K., Kraus, L., Fidzinski, P., Kornau, H., Dao, L., Wenke, N. K., Long, M., Rivalan, M., Winter, Y., Leubner, J., Herken, J., Mayer, S., Mueller, S., Boehm-Sturm, P., Dirnagl, U., Schmitz, D., Michael Kölch MD, Prüss, H. (2019). Human gestational *N* -methyl- d -aspartate receptor autoantibodies impair neonatal murine brain function. *Annals of Neurology*, ana.25552.

Kao, A. W., McKay, A., Singh, P. P., Brunet, A., & Huang, E. J. (2017). Progranulin, lysosomal regulation and neurodegenerative disease. *Nature Reviews Neuroscience*, *18*(6), 325–333.

King, D. J. (1998). Applications And Engineering Of Monoclonal Antibodies. *CRC Press*. https://books.google.de/books?id=LwdLBp3LzGAC&printsec=frontcover&hl=de&source=gbs_ge_summary_r&cad=0#v=onepage&q&f=false, last date accessed: 2020-05-13, 09.49am.

Kornau, H. C., Kreye, J., Stumpf, A., Fukata, Y., Parthier, D., Sammons, R. P., Imbrosci, B., Kurpjuweit, S., Kowski, A. B., Fukata, M., Prüss, H., & Schmitz, D. (2020). Human Cerebrospinal Fluid Monoclonal LGI1 Autoantibodies Increase Neuronal Excitability. *Annals of Neurology*, *87*(3), 405–418.

Kreye, J., Wenke, N. K., Chayka, M., Leubner, J., Murugan, R., Maier, N., Jurek, B., Ly, L. T., Brandl, D., Rost, B. R., Stumpf, A., Schulz, P., Radbruch, H., Hauser, A. E., Pache, F., Meisel, A., Harms, L., Paul, F., Dirnagl, U., Craig Garner, Dietmar Schmitz, Hedda Wardemann, Prüss, H. (2016). Human cerebrospinal fluid monoclonal N-methyl-D-aspartate receptor autoantibodies are sufficient for encephalitis pathogenesis. *Brain*, *139*(10), 2641–2652.

Kumar, A., Dhull, D. K., & Mishra, P. S. (2015). Therapeutic potential of mGluR5 targeting in

Alzheimer's disease. *Frontiers in Neuroscience*, *9*, 215.

Lancaster, E., Martinez-Hernandez, E., & Dalmau, J. (2011). Encephalitis and antibodies to synaptic and neuronal cell surface proteins. In *Neurology*, 77(2), 179–189.

Lau, C. G., & Zukin, R. S. (2007). NMDA receptor trafficking in synaptic plasticity and neuropsychiatric disorders. In *Nature Reviews Neuroscience* 8(6), 413–426.

LeBien, T. W., & Tedder, T. F. (2008). B lymphocytes: how they develop and function. *Blood*, *112*(5), 1570–1580.

Lefranc, M. P., Giudicelli, V., Ginestoux, C., Jabado-Michaloud, J., Folch, G., Bellahcene, F., Wu, Y., Gemrot, E., Brochet, X., Lane, J., Regnier, L., Ehrenmann, F., Lefranc, G., & Duroux, P. (2009). IMGT®, the international ImmunoGeneTics information system®. *Nucleic Acids Research*, 37(Database issue), D1006–D1012.

Leypoldt, F., Armangue, T., & Dalmau, J. (2015). Autoimmune encephalopathies. *Annals of the New York Academy of Sciences*, *1338*(1), 94–114

Louveau, A., Harris, T. H., & Kipnis, J. (2015). Revisiting the Mechanisms of CNS Immune Privilege. *Trends in Immunology*, *36*(10), 569–577.

Lubetzki, C., & Stankoff, B. (2014). Demyelination in multiple sclerosis. In *Handbook of Clinical Neurology* (Vol. 122, pp. 89–99). Elsevier B.V.

Ly, L.-T., Kreye, J., Jurek, B., Leubner, J., Scheibe, F., Lemcke, J., Wenke, N. K., Reincke, S. M., & Prüss, H. (2018). Affinities of human NMDA receptor autoantibodies: implications for disease mechanisms and clinical diagnostics. *Journal of Neurology*, *265*(11), 2625–2632.

Mabtech (2013). ELISA for human IgG. https://www.mabtech.com/sites/default/files/datasheets/3850-1AD-6.pdf, last date accessed: 2020-05-13, 8:50am.

Macherey-Nagel (2014). Plasmid DNA purification NucleoBond® Xtra Maxi. https://www.mn-net.com/media/pdf/ed/82/0f/Instruction-NucleoBond-Xtra.pdf, last date accessed: 2020-05-13, 8.54am.

Macherey-Nagel (2017). NucleoSpin® Gel and PCR Clean-up. https://www.takarabio.com/assets/documents/User%20Manual/NucleoSpin%20Gel%20and%20PCR%20Clean-up%20 User%20Manual_Rev_04.pdf, last date accessed: 2020-05-13, 09.06am.

Mao, L., Yang, L., Tang, Q., Samdani, S., Zhang, G., & Wang, J. Q. (2005). The scaffold protein Homer1b/c links metabotropic glutamate receptor 5 to extracellular signal-regulated protein kinase cascades in neurons. *The Journal of Neuroscience : The Official Journal of the Society for Neuroscience*, *25*(10), 2741–2752.

Mat, A., Adler, H., Merwick, A., Chadwick, G., Gullo, G., Dalmau, J. O., & Tubridy, N. (2013). Ophelia syndrome with metabotropic glutamate receptor 5 antibodies in CSF. *Neurology*, *80*(14), 1349–1350.

Melchers, F. (2015). Checkpoints that control B cell development. *The Journal of Clinical Investigation*, *125*(6), 2203–2210.

National Center for Biotechnology Information. IgBlast tool. https://www.ncbi.nlm.nih.gov/igblast/, last date accessed: 2020-05-13, 10.09am.

Oertel, W., & Schulz, J. B. (2016). Current and experimental treatments of Parkinson disease: A guide for neuroscientists. *Journal of Neurochemistry*, *139*, 325–337.

Petkau, T. L., Neal, S. J., Orban, P. C., MacDonald, J. L., Hill, A. M., Lu, G., Feldman, H. H., Mackenzie, I. R. A., & Leavitt, B. R. (2010). Progranulin expression in the developing and adult murine brain. *The Journal of Comparative Neurology*, *518*(19), 3931–3947.

Platt, M. P., Agalliu, D., & Cutforth, T. (2017). Hello from the other side: How autoantibodies circumvent the blood-brain barrier in autoimmune encephalitis. In *Frontiers in Immunology*, 8, 442.

Ribeiro, F. M., Paquet, M., Ferreira, L. T., Cregan, T., Swan, P., Cregan, S. P., & Ferguson, S. S. G. (2010). Metabotropic glutamate receptor-mediated cell signaling pathways are altered in a mouse model of Huntington's disease. *The Journal of Neuroscience : The Official Journal of the Society for Neuroscience*, *30*(1), 316–324.

Rolink, A. G., Andersson, J., & Melchers, F. (1998). Characterization of immature B cells by a novel monoclonal antibody, by turnover and by mitogen reactivity. *European Journal of Immunology*, *28*(11), 3738–3748.

Romano, C., Sesma, M. A., McDonald, C. T., O'malley, K., van den Pol, A. N., & Olney, J. W. (1995). Distribution of metabotropic glutamate receptor mGluR5 immunoreactivity in rat brain. *The Journal of Comparative Neurology*, *355*(3), 455–469.

Ryan, C. L., Baranowski, D. C., Chitramuthu, B. P., Malik, S., Li, Z., Cao, M., Minotti, S., Durham, H. D., Kay, D. G., Shaw, C. A., Bennett, H. P. J., & Bateman, A. (2009). Progranulin is expressed within motor neurons and promotes neuronal cell survival. *BMC Neuroscience*, *10*, 130.

Sanderson, R. D., Lalor, P., & Bernfield, M. (1989). B lymphocytes express and lose syndecan at specific stages of differentiation. *Cell Regulation*, *1*(1), 27–35.

Sergin, I., Jong, Y.-J. I., Harmon, S. K., Kumar, V., & O'Malley, K. L. (2017). Sequences within the C Terminus of the Metabotropic Glutamate Receptor 5 (mGluR5) Are Responsible for Inner Nuclear Membrane Localization. *The Journal of Biological Chemistry*, *292*(9), 3637–3655.

Shigemoto, R., Nomura, S., Ohishi, H., Sugihara, H., Nakanishi, S., & Mizuno, N. (1993). Immunohistochemical localization of a metabotropic glutamate receptor, mGluR5, in the rat brain. *Neuroscience Letters*, *163*(1), 53–57.

Shin, Y.-W., Lee, S.-T., Park, K.-I., Jung, K.-H., Jung, K.-Y., Lee, S. K., & Chu, K. (2018). Treatment strategies for autoimmune encephalitis. *Therapeutic Advances in Neurological Disorders*, *11*, 1756285617722347.

Sigma-Aldrich. (2013). *ANTI-FLAG M2 Magnetic Beads*. https://www.sigmaaldrich.com/content/dam/sigma-aldrich/docs/Sigma/Bulletin/m8823bul.pdf, last date accessed: 2020-05-13, 09.31am

Smith, K. R., Damiano, J., Franceschetti, S., Carpenter, S., Canafoglia, L., Morbin, M., Rossi, G., Pareyson, D., Mole, S. E., Staropoli, J. F., Sims, K. B., Lewis, J., Lin, W.-L., Dickson, D. W., Dahl, H.-H., Bahlo, M., & Berkovic, S. F. (2012). Strikingly different clinicopathological phenotypes determined by progranulin-mutation dosage. *American Journal of Human Genetics*, *90*(6), 1102–1107.

Spatola, M., Sabater, L., Planagumà, J., Martínez-Hernandez, E., Armangué, T., Prüss, H., Iizuka, T., Caparó Oblitas, R. L., Antoine, J.-C., Li, R., Heaney, N., Tubridy, N., Munteis Olivas, E., Rosenfeld, M. R., Graus, F., & Dalmau, J. (2018a). Encephalitis with mGluR5 antibodies: Symptoms and antibody effects. *Neurology*, *90*(22), e1964–e1972.

Spatola, M., Sabater, L., Planagumà, J., Martínez-Hernandez, E., Armangué, T., Prüss, H., Iizuka, T., Caparó Oblitas, R. L., Antoine, J.-C., Li, R., Heaney, N., Tubridy, N., Munteis Olivas, E., Rosenfeld, M. R., Graus, F., & Dalmau, J. (2018b). Encephalitis with mGluR5 antibodies. *Neurology*, *90*(22), e1964–e1972.

Theofilopoulos, A. N., Kono, D. H., & Baccala, R. (2017). The multiple pathways to autoimmunity. *Nature Immunology*, *18*(7), 716–724.

Thurner, L., Preuss, K.-D., Fadle, N., Regitz, E., Klemm, P., Zaks, M., Kemele, M., Hasenfus, A., Csernok, E., Gross, W. L., Pasquali, J.-L., Martin, T., Bohle, R. M., & Pfreundschuh, M. (2013). Progranulin antibodies in autoimmune diseases. *Journal of Autoimmunity*, *42*, 29–38.

Tiller, T., Meffre, E., Yurasov, S., Tsuiji, M., Nussenzweig, M. C., & Wardemann, H. (2008). Efficient generation of monoclonal antibodies from single human B cells by single cell RT-PCR and expression vector cloning. *Journal of Immunological Methods*, *329*(1–2), 112–124.

Torigoe, M., Iwata, S., Nakayamada, S., Sakata, K., Zhang, M., Hajime, M., Miyazaki, Y., Narisawa, M., Ishii, K., Shibata, H., & Tanaka, Y. (2017). Metabolic Reprogramming Commits Differentiation of Human CD27 + IgD + B cells to Plasmablasts or CD27 − IgD − Cells . *The Journal of Immunology*, *199*(2), 425–434.

Van Regenmortel, M. H. V. (2014). Specificity, polyspecificity, and heterospecificity of antibody-antigen recognition. *Journal of Molecular Recognition*, *27*(11), 627–639.

Wang, H.-Y., MacDonald, M. L., Borgmann-Winter, K. E., Banerjee, A., Sleiman, P., Tom, A., Khan, A., Lee, K.-C., Roussos, P., Siegel, S. J., Hemby, S. E., Bilker, W. B., Gur, R. E., & Hahn, C.-G. (2018). mGluR5 hypofunction is integral to glutamatergic dysregulation in schizophrenia. *Molecular Psychiatry*, 25(4), 750-760.

Wang, P., & Wilson, S. R. (2013). Mass spectrometry-based protein identification by integrating de novo sequencing with database searching. *BMC Bioinformatics*, *14*(Suppl 2), S24.

Wardemann, H., Yurasov, S., Schaefer, A., Young, J. W., Meffre, E., & Nussenzweig, M. C. (2003). Predominant Autoantibody Production by Early Human B cell Precursors. *Science*, *301*(5638), 1374 LP – 1377.

Warrington, A. E., Bieber, A. J., Ciric, B., Pease, L. R., Van Keulen, V., & Rodriguez, M. (2007). A recombinant human IgM promotes myelin repair after a single, very low dose. *Journal of Neuroscience Research*, *85*(5), 967–976.

Yin, F., Dumont, M., Banerjee, R., Ma, Y., Li, H., Lin, M. T., Beal, M. F., Nathan, C., Thomas, B., & Ding, A. (2010). Behavioral deficits and progressive neuropathology in progranulin-deficient mice: a mouse model of frontotemporal dementia. *FASEB Journal : Official Publication of the Federation of American Societies for Experimental Biology*, *24*(12), 4639–4647.

Zhou, Y., & Danbolt, N. C. (2014). Glutamate as a neurotransmitter in the healthy brain. In *Journal of Neural Transmission*, *121*(8), 799-817.

Zlokovic, B. V. (2008). The blood-brain barrier in health and chronic neurodegenerative disorders. *Neuron*, *57*(2), 178–201.

Statutory Declaration

"I, Sarah Lina Kurpjuweit, by personally signing this document in lieu of an oath, hereby affirm that I prepared the submitted dissertation on the topic *Generation of Monoclonal Antibodies against the Metabotropic Glutamate Receptor 5 and Progranulin in Autoimmune Encephalitis and a Potential Approach to Remedy Antibody Effects*, independently and without the support of third parties, and that I used no other sources and aids than those stated.

All parts which are based on the publications or presentations of other authors, either in letter or in spirit, are specified as such in accordance with the citing guidelines. The sections on methodology (in particular regarding practical work, laboratory regulations, statistical processing) and results (in particular regarding figures, charts and tables) are exclusively my responsibility.

Furthermore, I declare that I have correctly marked all of the data, the analyses, and the conclusions generated from data obtained in collaboration with other persons, and that I have correctly marked my own contribution and the contributions of other persons. I have correctly marked all texts or parts of texts that were generated in collaboration with other persons.

My contributions to any publications to this dissertation correspond to those stated in the below joint declaration made together with the supervisor. All publications created within the scope of the dissertation comply with the guidelines of the ICMJE (International Committee of Medical Journal Editors; www.icmje.org) on authorship. In addition, I declare that I shall comply with the regulations of Charité – Universitätsmedizin Berlin on ensuring good scientific practice.

I declare that I have not yet submitted this dissertation in identical or similar form to another Faculty.

The significance of this statutory declaration and the consequences of a false statutory declaration under criminal law (Sections 156, 161 of the German Criminal Code) are known to me."

Date Signature

Declaration of Contribution to any Publications

Sarah Lina Kurpjuweit contributed the following publication:

Kornau, H. C., Kreye, J., Stumpf, A., Fukata, Y., Parthier, D., Sammons, R. P., Imbrosci, B., Kurpjuweit, S., Kowski, A. B., Fukata, M., Prüss, H., & Schmitz, D. (2020). Human Cerebrospinal Fluid Monoclonal LGI1 Autoantibodies Increase Neuronal Excitability. *Annals of Neurology*, *87*(3), 405–418.

Contribution: Sarah Lina Kurpjuweit contributed to the acquisition and analysis of data; in particular to the workup of CSF samples including cell staining and fluorescence-activated cell sorting.

_____

Signature, date and stamp of first supervising university professor / lecturer

_____

Signature of doctoral candidate

List of Publications

Kornau, H. C., Kreye, J., Stumpf, A., Fukata, Y., Parthier, D., Sammons, R. P., Imbrosci, B., Kurpjuweit, S., Kowski, A. B., Fukata, M., Prüss, H., & Schmitz, D. (2020). Human Cerebrospinal Fluid Monoclonal LGI1 Autoantibodies Increase Neuronal Excitability. *Annals of Neurology*, *87*(3), 405–418.

Mein Lebenslauf wird aus datenschutzrechtlichen Gründen in der elektronischen Version meiner Arbeit nicht veröffentlicht.

Acknowledgments

Firstly, I would like to thank my supervisor Harald Prüß for enabling this project and for the trust placed in me.

Special thanks go to Jakob Kreye for the initial training, the supervision and for always providing a positive atmosphere.

I would like to thank Betty Jurek, Hans-Christian Kornau and Doreen Brandl for their advice and their patience when answering my questions.

For both the financial and the intellectual support I thank the Studienstiftung des deutschen Volkes.

To my fellow lab mates Marie-Luise Machule and Le-Minh Dao, thank you for the time spent together and the friendship that has developed from it.